Nanoscale

Accepted Manuscript

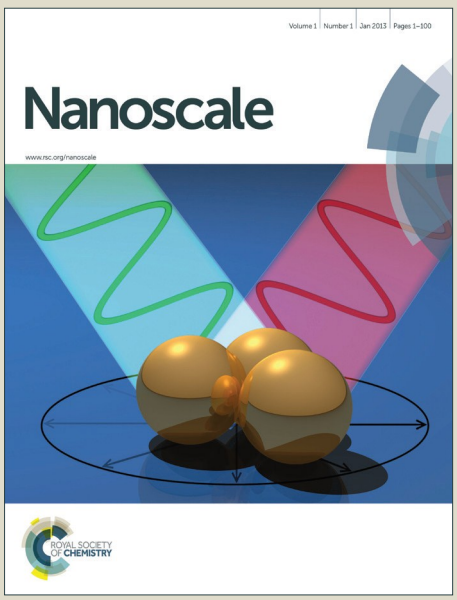

ROYAL SOCIETY OF CHEMISTRY

www.rsc.org/nanoscale

Nanoscale Guidelines to Referees

Nanoscale **(www.rsc.org/nanoscale)** is a community-spanning journal publishing very high quality, high impact research across nanoscience and nanotechnology.

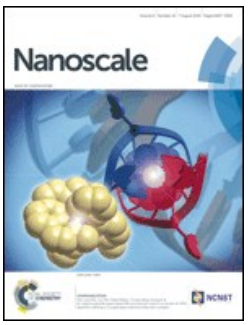

Nanoscale's latest Impact Factor is 7.394

We aspire to even higher values in future years

Nanoscale Associate Editors stress very high standards for acceptance in the journal. Articles must report extremely novel, very high quality, reproducible new work of broad general interest.

As a referee, our Associate Editors strongly encourage you to recommend only the best work for publication in *Nanoscale*. Since launch in late 2009, *Nanoscale* has quickly become a leading journal. We aspire for the journal to publish truly world-class research.

Routine, limited novelty or incremental work – even if competently researched and reported - should **not** be recommended for publication. ***Nanoscale*** **demands high novelty and high impact**.

We strongly discourage fragmentation of work into several short publications. Unnecessary fragmentation is a valid reason for rejection.

Thank you very much for your assistance in evaluating this manuscript, which is greatly appreciated.

With our best wishes,

Chunli Bai (Editor-in-Chief)

Xiaodong Chen, Serena Corr, Yves Dufrêne, Andrea Ferrari, Dirk Guldi, Xingyu Jiang, RongChao Jin, Yamuna Krishnan, Jie Liu, Xiaogang Liu, Wei Lu, Francesco Stellacci, Shouheng Sun, Jianfang Wang, Hongxing Xu, Xiao Cheng Zeng (Associate Editors)

General Guidance (For further details, see the Royal Society of Chemistry's Refereeing Procedure and Policy**)**

Referees have the responsibility to treat the manuscript as confidential. Please be aware of our **Ethical Guidelines** which contain full information on the responsibilities of referees and authors.

When preparing your report, please:
• Comment on the originality, importance, impact and scientific reliability of the work;
• State clearly whether you would like to see the paper accepted or rejected and give detailed comments (**with references**) that will both help the Editor to make a decision on the paper and the authors to improve it;

Please inform the Editor if:
• There is a conflict of interest;
• There is a significant part of the work which you are not able to referee with confidence;
• If the work, or a significant part of the work, has previously been published, including online publication, or if the work represents part of an unduly fragmented investigation.

When submitting your report, please:
• Provide your report rapidly and within the specified deadline, or inform the Editor immediately if you cannot do so. We welcome suggestions of alternative referees.

If you have any questions about reviewing this manuscript, please contact the Editorial Office at **nanoscale@rsc.org**

Dear referees,

Attached please find the revised manuscript NR-COM-12-2015-008596 entitled "Ultrasound-responsive ultrathin multiblock copolyamide vesicles". Thank you very much for giving us a chance to improve the manuscript. During the revisions, we had supplemented transmission electron microscopy (TEM) and fluorescence data as well as some references to further improve the manuscript. We have responded all your comments and have indicated all the changes made in the manuscript. The detailed responses to you are shown as follows.

To referee 1

Comments: Zhou and co-workers present a very interesting article. The authors have addressed all the referees' comments. The article presents a novel method to specifically deliver therapeutic agents and the data (after corrections) support the conclusions. I believe this is an interesting method. I will suggest minor changes. In conclusion, a very nice contribution which I believe it will find lot of interest in the readership of Nanoscale. I strongly recommend publication as it is or after minor corrections.

Response to the comments: The authors feel greatly thankful to referee 1 for the positive comments on the manuscript and we have addressed all the points noted by the referee. The point-to-point responses are shows as follows.

Question 1: Sentence "Different from diblock copolymers .... blocks" i think could be deleted it is a bit obvious

Answer 1: Thank the referee for the careful reminder. We have deleted this sentence in the manuscript and added a new statement in the revised manuscript in order to better connect the two paragraphs (sentence in red in the second paragraph of page 1).

Question 2: dimension of wall 4.5 nm, maybe an incertitude range could be included.

Answer 2: The referee is right. The wall thickness is 4.3 ± 0.4 nm through the statistical analyses of 30 particles (the blue sentence in the second paragraph of page 2).

Question 3: I will add in the comparison with other stimuli systems, the use of Alternated magnetic field, as it is one of the most investigated. Perhaps, the following

papers could be cited: Angewandte Chemie 125 (52), 14402-14406; Polymer Chemistry 5 (10), 3311-3315; Langmuir 30 (34), 10493-10502.

Answer 3: We have added the comparison with alternated magnetic field (words in purple in the third paragraph of page 1) and also cited these three papers in the reference 8.

To Referee 2

Comments: The manuscript describes synthesis, processes of self-assembly and ultrasound-induced opening of novel polymer multiblock vesicles. Main advantages of the vesicles developed by the authors are interesting morphology, relative ease of formation, and ultrathin vesicle walls, which in its turn would lead to more efficient "drug release" upon ultrasound treatment. Moreover, the authors carried out immense amount of work, and the whole study feels well-done: all hypotheses are confirmed by a large array of methods, including DRS measurements, calorimetric methods, microscopy techniques, computer modeling, etc., figures are illustrative, and selection of references is up to date.

In my opinion, additions to the manuscript after the first peer-review fully cover the questions made by the previous referees. Additions of the authors are also useful for better comprehension of the main concepts of the study. Despite minor concerns, I recommend this manuscript to be accepted to Nanoscale journal of The Royal Society of Chemistry, as I deem it quite innovative and interesting to a broad spectrum of specialists in chemistry and materials science dealing with polymer colloid chemistry, self-assembled vesicle formation, drug delivery systems, dissipative particle dynamics simulation, etc.

Response to the comments: Thank the referee for the positive comments, and we have addressed all the questions as noted by the referee. The point-to-point responses are shows as follows.

Question 1: The authors correctly assume that dye molecules not located inside the vesicles will have higher values of fluorescence intensity due to the absence of the aggregation induced quenching in the experiment that demonstrates release of nile red dye upon ultrasonication of the vesicle solutions. Although, it would be more illustrative to provide comparison of the concentration-dependent fluorescence intensity values of NR dye solution with the values obtained upon vesicle disruption. Moreover, such comparison could lead to quantification of the drug release since estimative concentration of the dye in the vesicles is known.

Answer 1: We are really sorry for the misleading. In fact, a quenching of fluorescence would be observed if NR was released into water due to an aggregation induced

quenching effect. As shown in the following two figures, there is almost no fluorescence for the NR in water (black curve in figure 1a and the magnified one in figure 1b). However, if the NR was encapsulated in the hydrophobic layers of MBCPA vesicles, a pronounced fluorescence was observed, and a clear decrease of fluorescence was observed after the ultrasound irradiation of the vesicle for 14 min (Figure 1a). Thus, it is reasonable to detect the release of NR from the vesicles by measuring the changes of fluorescence since the fluorescence of the released NR is negligible.

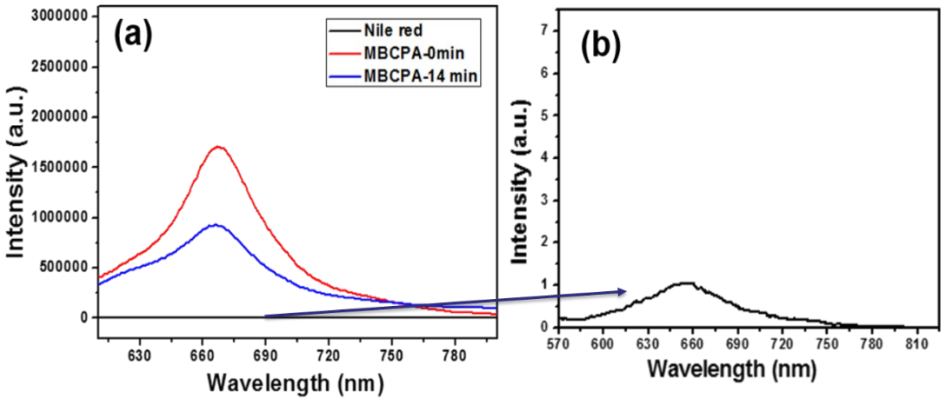

Figure 1 (a) The fluorescence emission spectra (excitation: 600nm) of NR dyes in water, NR-loaded MBCPA vesicles (MBCPA-0min) and the vesicles after ultrasonic irradiation for 14 min (MBCPA-14min); (b) The magnified fluorescence curve of NR dyes.

Question 2: Despite fluorescence studies performed in this work being complete and conclusive, it also could be demonstrative and providing further evidence for the pathway of vesicle "opening" to carry out TEM (or/and AFM) imaging of the sample after sonication.

Answer 2: Thank the referee for the kind suggestion. We had supplemented the TEM image of the self-assemblies after the sonication treatment of the vesicles in the revised supporting information (Fig. S9, ESI†), which indicates the vesicles were disrupted by ultrasonication into fragments. We had also pointed it out in the revised main text (sentences in green in the second paragraph of page 4)

Question 3: TEM images show a large number of vesicles with holes. It is not clear what is statistical percentage of these "not-complete" vesicles, and how they affect reproducibility of the drug release tests, if their amount varies from synthesis to synthesis. Most importantly, although computer modeling clearly shows a stage of the vesicle formation, where a hole is present, it is not discussed by the authors, why part of the sample remains this way and does not progress further until vesicle is fully formed. The nature of these holes could be explained by the multiblock nature of the aggregate, but, in my opinion, this moment deserves more focus in the main text of the article.

Answer 3: We are really sorry for the misleading. In fact, the finally obtained vesicles are completely closed and very stable in water. No release of NR was observed from the vesicles without ultrasonication (Fig. 5b), which also proved the vesicles were complete. Only a small amount of the vesicles with holes were observed, which was probably caused by the disruption of vesicles due to the evaporation of water during the sampling process for TEM measurement. We just wanted to prove the hollow structure of the vesicles by selecting a TEM image of vesicles with holes (Figure 2a in the previous version and Fig. S5 in the ESI† of this new version); however, it could not represent the true morphology of the vesicles and would certainly mislead the readers. Thus, during the revision, we decided to replace this misleading TEM image with a new one consisting of complete vesicles (Fig. 2a of this version). In addition, we also revised the explanations of Fig. 2a in the revised main text (sentences in orange in the second paragraph of page 2). Thank the referee for the kind reminder. We are really sorry for such a misleading.

Question 4: When the authors list power of the ultrasound employed for vesicle disruption on page 11, they use "150 W", it would be more proper to list the intensity of the ultrasound (W/cm^2) also, since it is a more known unit for specialists dealing with drug release systems.

Answer 4: Thank the referee for the professional advice. However, we feel very sorry for the absence of intensity of ultrasound (W/cm^2), because we do not have a device to measure the data for our ultrasound instrument. So we list the power and frequency of our ultrasound instrument in the manuscript. We also noted that, some investigations on the release from vesicles triggered by ultrasound also just provide the data of power and frequency (Reference 9). Anyway, we are really sorry for this.

Question 5: The text on Fig. 2d is a little too small for comfortable reading. The text "membrane thickness", as well as legend text on Fig. 4b are too small. This also applies to the legend caption of Fig. 5a.

Answer 5: The referee is right, and we have revised all these flaws in the Figures of the revised version.

Dear referees, thank you again for your important and thoughtful suggestions on the further revision of our manuscript. We hope the revised manuscript is more satisfactory.

With best wishes,

Sincerely yours

Prof. Dr. Yongfeng Zhou
School of Chemistry and Chemical Engineering
Shanghai Jiao Tong University
800 Dongchuan Road, Shanghai 200240
People's Republic of China
Email: yfzhou@sjtu.edu.cn,
Tel: +86-21-54742664
Fax: +86-21-54741297

Journal Name

COMMUNICATION

Ultrasound-responsive ultrathin multiblock copolyamide vesicles

Lei Huang,[a] Chunyang Yu,[b] Tong Huang,[b] Shuting Xu,[b] Yongping Bai,[a*] and Yongfeng Zhou[b*]

Received 00th January 20xx,
Accepted 00th January 20xx

DOI: 10.1039/x0xx00000x

www.rsc.org/

This study reports the self-assembly of a novel polymer vesicles from an amphiphilic multiblock copolyamide, and the vesicles have shown a special structure of ultrathin wall thickness of about 4.5 nm and of a combined bilayer and monolayer packing model. Most interestingly, the vesicles are ultrasound-responsive and can release the encapsulated model drugs in response to ultrasonic irradiation.

Among all fantastic supramolecular self-assemblies, vesicles including lipid vesicles (liposomes), surfactant vesicles and polymer vesicles (polymersomes) have drawn great attention due to their great importance in living systems and various applications such as in pharmaceutical, diagnostic, and cosmetic agents.[1] Up to now, polymer vesicles have been obtained from the self-assembly of many kinds of polymer architectures like diblock copolymers, triblock copolymers, star copolymers, graft copolymers, dendrimers and hyperbranched polymers, and have demonstrated great potentials from both the scientific and industrial communities.[2] Herein, we report for the first time on a novel polymer vesicles self-assembled from multiblock copolymers.

As we know, multiblock copolymers are a kind of linear polymers consisting of more than three polymer blocks.[3] Thus, in principle, such a kind of polymer structure can not only enlarge the structural diversity of polymers but also allow the incorporation of more functionalities in one polymer chain.[4] In addition, from the self-assembly aspect, multiblock copolymers can introduce multiple hydrophilic and hydrophobic segments in the polymer chains, which will induce more complex chain folding and phase separation processes when compared with those of diblock or triblock copolymers and then may generate more complicated supramolecular structures. It has been even considered as a simple model for protein folding and DNA packing.[5] However, despite of these advantages, the studies on

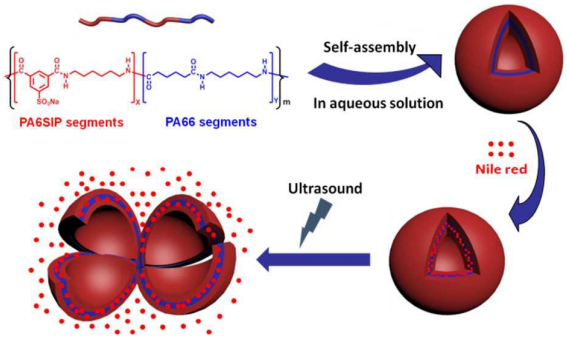

Scheme 1 Synthesis and self-assembly of multiblock copolyamides into ultrasound-responsive vesicles.

the synthesis and self-assembly of multiblock copolymers are still great limited. Among them, Halperin, Wang and Lu et al.[5,6] have performed the computer simulations, while Tan and Sommerdijk et al[7] have conducted the experimental studies. Nevertheless, the obtained self-assemblies are generally limited to micelles.

Herein, as a new progress, we report the self-assembly of vesicles from a multiblock copolyamide (MBCPA, Scheme 1) in water. The obtained vesicles have an ultrathin wall of 4.5 nm. Most interestingly, they can be disrupted and release the encapsulated hydrophobic nile red in response to ultrasonic irradiation. Compared to other stimuli such as pH, oxidation/reduction, temperature, light, alternated magnetic field and electrical field etc., noninvasive ultrasound may possess some unique advantages such as penetrating deeply in the body, relatively easy dynamic examination, providing high resolution images of the soft tissues, easily accessible and low cost etc.[8] Up to now, only few works have been reported on the ultrasound-responsive polymer vesicles generating from the self-assembly of poly(ethylene oxide)-block-poly[2-(diethylamino) ethyl methacrylate- statistical-2-tetrahydrofuranyloxy ethyl methacrylate] (PEO-b- P(DEA-stat-TMA)) and poly (ethylene glycol)-polyactide (PEG-b- PDLLA),[9] and thus the present work represents a new type of the ultrasound-responsive polymer vesicles.

The MBCPAs used here were synthesized by solution polycondensation in two steps following the reaction method

[a] School of Chemical Engineering and Technology, Harbin Institute of Technology, Harbin 150001, PR China. Email: baifengbai@hit.edu.cn
[b] School of Chemistry and Chemical Engineering, State Key Laboratory of Metal Matrix Composites, Shanghai Jiao Tong University, 800 Dongchuan Road, Shanghai 200240, China. Fax: (+86) 21 54741297; Email: yfzhou@sjtu.edu.cn

† Electronic Supplementary Information (ESI) available: details of experiments and characterization, and FT-IR, TEM, DPD, FL and micro-DSC results. See DOI: 10.1039/x0xx00000x

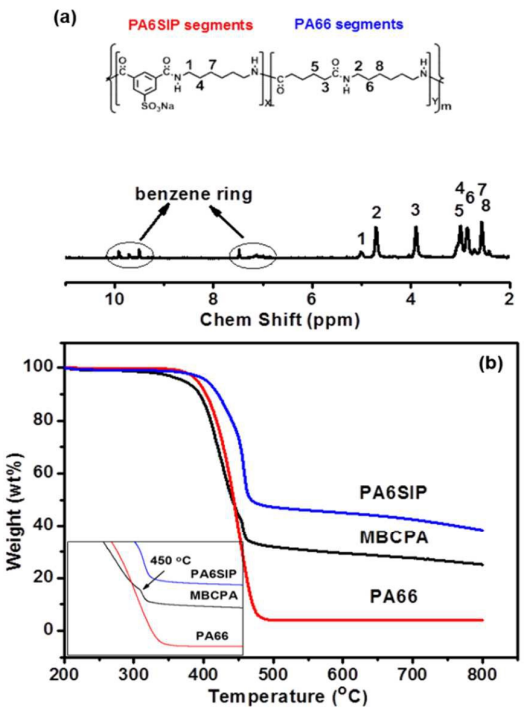

Fig. 1 Characterizations of as-prepared MBCPAs. (a) The NMR spectrum; (b) The TGA curves.

described (Fig. S1, ESI†) by Yamazaki.[10] In the first step, poly (Sodium 5-sulfoisophthalate-alt-hexamethylenediamine) (PA6SIP) and poly (hexanedioic acid-alt-hexamethylenediamine) (PA66) segments were synthesized, respectively; in the second step, the multiblock copolyamide was synthesized by coupling of these two segments. Fig. 1a shows the ^{1}H NMR spectrum of the synthesized MBCPA along with peak assignments in deuterated sulfuric acid. The signals appearing in the region of 6.0-10.0 ppm are ascribed to the protons of benzene ring, and the signals at about 5.0 ppm (peak 1), 4.7 ppm (peak 2) and 3.9 ppm (peak 3) come from the protons adjacent to the amide groups. The chemical shifts below 3.2 ppm are assigned to the methylene moieties (peaks 4-8). Moreover, the peak 2 is an independent signal assigned to the PA66 segments, while the peak 1 is the independent proton signals for PA6SIP segments. The real composition ratio of MBCPA (PA6SIP:PA66) can be obtained according to the integrated areas of peak 1 (S1), peak 2 (S2), and is about 0.35:1. According to Carothers' equation, there should be 4 PA6SIP blocks and 10 PA66 blocks in each MBCPA in theory. So the real composition ratio between PA6SIP and PA66 blocks in MBCPA (0.35:1) is comparable to the theoretic one (0.4:1). The multiblock structure of the synthesized copolyamide was also proved by the thermal gravity analysis (TGA, Fig. 1b), and the TGA curve of MBCPAs shows two stages of evident mass loss at 400 °C due to degradation of the PA66 blocks and at 450 °C due to degradation of the PA6SIP blocks (inset in Fig. 1b).[10] Differential scanning calorimetry (DSC) traces shows two melting peaks around 229 °C and 258 °C for the physical blend of PA66 and PA6SIP, while only one melting peak around 252 °C for MBCPAs, which further ascertain the multiblock structure of MBCPAs (Fig. S4, ESI†). The intrinsic viscosity measured in sulfuric acid (96 wt %) by an Ubbelohde viscometer at 30 °C is

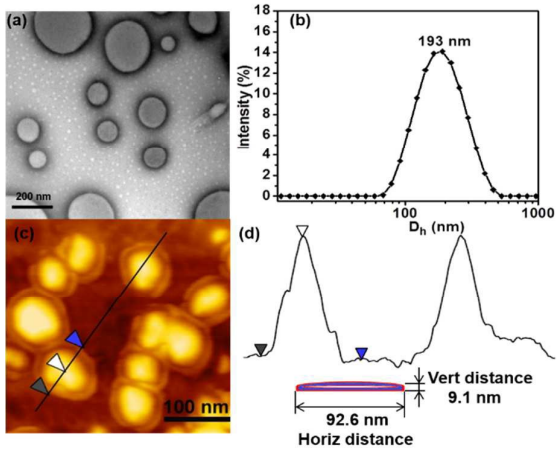

Fig. 2 Morphology characterizations of MBCPA self-assemblies. (a)The TEM image of MBCPA self-assemblies stained by phosphotungstic acid; (b)The DLS curve; (c)The AFM image; (d) The sectional height profiles of the particles and the cartoon to illustrate the cross section of the particles.

1.42, and the viscosity-average molecular weight is about 11,672 according to the semiempirical equation (Fig. S2, ESI†) generated by Ruijter and Picken.[10] The FTIR measurements provide a further evidence to prove the formation of multiblock copolyamides (Fig. S3, ESI†).

In the as-prepared MBCPAs, the PA66 segments are hydrophobic, while the benzene sulfonic acid sodium groups in PA6SIP segments are hydrophilic, so MBCPAs are amphiphilic in nature. Moreover, the amide groups in MBCPAs are subject to form intermolecular hydrogen bonds. So the self-assembly ability of MBCPAs are well expected. To prove this, a direct hydration method by putting polymers into deionized water with a typical concentration of 1 mg/mL was used to trigger the self-assembly process. The transmission electron microscopy (TEM) images (Fig. 2a) show the aggregates are spherical particles with a clear contrast difference between the inner pool and the outer black thin wall. In addition, the particles with holes can also be observed (Fig. S5, ESI†). These results indicate that the aggregates might be vesicles with hollow lumens. The vesicle wall thickness is around 4.3 ± 0.4 nm through the statistical analyses of 30 particles. The dynamic light scattering measurement indicates the vesicles have an average hydrodynamic diameter around 193 nm with a PDI of 0.16 (Fig. 2b). The atomic force microscopy (AFM) image (Fig. 2c) shows collapsed particles with the height-to-diameter ratio more than 1:10, which also proves the formation of vesicles. The height of the collapsed vesicles is around 9 nm, which is equal to the thickness of two stacked vesicle membrane as shown in the cartoon (Fig. 2d). Thus, the vesicle wall thickness measured by TEM is in good agreement with that measured by AFM. The MBCPA vesicles have a polydisperse size distribution according to the TEM, AFM and DLS measurements. In fact, a wide size distribution is often observed for the vesicles self-assembled by a direct hydration method.[11]

The above experiments reveal that the multiblock polyamides could self-assemble into vesicles in aqueous solution, so what is the self-assembly mechanism? To address it, a dissipative particle dynamics simulation was performed to explore the self-

assembly process of the as-prepared MBCPAs. In order to capture the essential feature of MBCPAs, a model molecule $[(AB)_2(CB)_5]_3$ was constructed in the DPD simulations (Fig. 3a). In this system, one "A" bead represents a hydrophilic benzene sulfonic acid sodium group, one "B" bead refers to a hydrophobic hexamethylenediamine group, while one "C" bead refers to a hydrophobic adipic acid group (Fig. 3a). Thus, $(AB)_2$ represents a PA6SIP blocks, while $(CB)_5$ represents a PA66 block. The ratio between AB to CB is 2:5 (0.4:1), which is a mimic of the theoretic composition of MBCPAs. For easy handling, a multiblock polymer with 3 degree of polymerization was constructed in our DPD model. The details of the simulation model and method are described in the Supporting Information. Fig. 3 displays snapshots of the self-assembly process through the DPD simulation. After the initially random state (Fig. 3b), the MBCPA molecules aggregated into a large irregular aggregate with lamellar structure at 66 ns (Fig. 3c). Then, the large irregular aggregate gradually changed to a hollow vesicular shape with several holes throughout the vesicle membrane at 132 ns (Fig. 3d). The vesicle turned more regular with the holes closing from 198 ns (Fig. 3e), 248 ns (Fig. 3f) to 300 ns (Fig. 3g). At t = 792 ns, the vesicle was completely sealed with a regular globular shape (Fig. 3h). Generally, the vesicles from the linear block copolymers can be generated through the mechanisms of "micelle-rod-membrane-vesicles" or "micelle-semivesicle-vesicle".[12] The mechanism of MBCPA vesicles as shown here is closer to the "micelle-rod-membrane-vesicle" process except that no rod-like intermediates are observed, and it is very similar to the vesicle self-assembly mechanism from Janus dendrimers and Janus hyperbranched polymers.[13] During the TEM measurements, some intermediates of lamellar structures, vesicles with two or more holes, and vesicles in closing the holes were also observed (Fig. S6, ESI†), which agree well with the self-assembly pathway as indicated in Fig. 3.

In addition, the simulation results can further provide details on the vesicle structure. Fig. 4a shows that the polymer adopts a core-shell structure with the hydrophilic units on the vesicle shells and with the hydrophobic units inside the vesicle cores. In addition, it can be also seen that the polymer chains display three kinds of packing behaviors in the vesicle membrane (Fig. 4a), namely the folding chains, hanging chains and spanned chains, respectively. For folding chains, the polymer segments do not span the whole vesicle membrane but fold into a "v" type inside the membrane; For spanned chains, the polymer segments do span the whole vesicle membrane; For hanging chains, the polymer segments do not fold and span the vesicle, but just hang in the vesicle membrane. Through the combination of these three packing models, the MBCPAs pack into the vesicles. So, the vesicle is not a simple monolayer or bilayer structure, on the contrary, it is a combination of bilayer and monolayer structure. Such a self-assembly mechanism might be a unique characteristics for multiblock copolymer vesicles when compared to that of the conventional polymersomes and liposomes.[14]

Furthermore, the density distribution from the center of mass to the outside of the vesicle was calculated to characterize the vesicle microstructure. The detailed calculation description can be seen in supporting information. As can be seen in Fig. 4b, the density distribution profile of hydrophilic segments has two

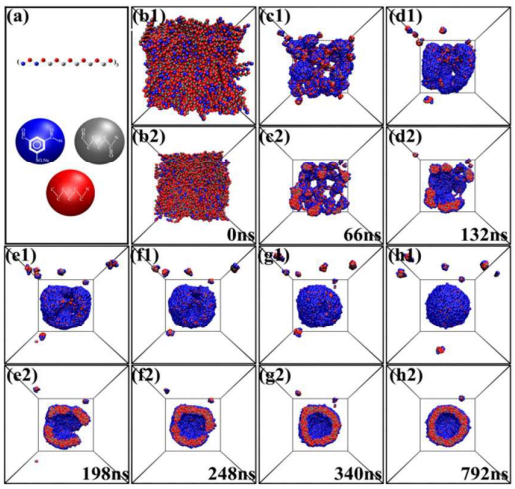

Fig. 3 DPD simulations on the self-assembly of MBCPAs captured at different time intervals. (a) The model $[(AB)_2(CB)_5]_3$ for one MBCPA molecule. (b) Randomly distributed $[(AB)_2(CB)_5]_3$ molecules in water. (c and d) Formation of a large irregular aggregate with the lamellar structure. (e) Formation of a hollow vesicular aggregate with several holes throughout the vesicle membrane. (f and g) The vesicle in closing the holes. (h) The final vesicle structure. For each image from (b–h), the upper one is the 3D view, while the lower one is the cross-section view. The water beads are removed for clarity. Blue: A type bead (benzene sulfonic acid sodium salt block); red: B type bead (hexamethylenediamine block); gray: C type bead (adipic acid block).

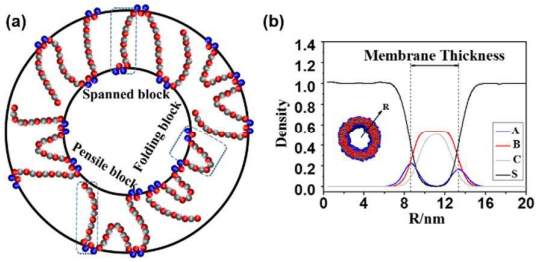

Fig. 4 The vesicular structure by the DPD simulation. (a) The schematic of the packing modes of polymer chains within the vesicle membrane, abd the circle represents the membrane of the vesicle. (b) Radial density distributions of the A (blue), B (red), C (gray) and S (black, solvent particle) components in the vesicle. The distance from the center of mass of the vesicle to the outside of the vesicle is R. Membrane thickness is defined as the distance between the peaks of density distribution of the hydrophilic A segments located on the inside surface and on the outside surface.

peaks while the density distribution profile of two hydrophobic blocks has only one smooth peak, which supports the core-shell structure very well. We can also calculate the membrane thickness of the vesicles from the density distribution profile. The calculated membrane thickness of the vesicle is 4.5 nm, which is very close to the experimental result 4.3 ± 0.4 nm.

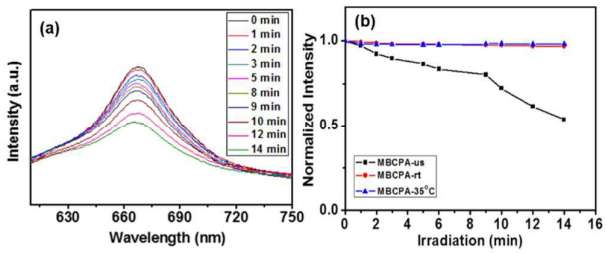

Fig. 5 Ultrasound-responsive dye release experiments from vesicles. (a)The fluorescence emission spectra of NR-loaded MBCPA vesicles (excitation: 600nm) recorded at different ultrasonic irradiation time; (b)The accumulative release of NRs from MBCPA vesicles with (MBCPA-us) or without ultrasonication that performed at room temperature (MBCPA-rt) or at 35 ^{o}C (MBCPA-35 ^{o}C), respectively.

Generally, the vesicle thickness of polymersomes is around 10-30 nm, while that of the liposomes is around 5 nm or less.[15] Thus, as a kind of polymer vesicles, the wall thickness of 4.5 nm for the obtained MBCPA vesicles is ultrathin. And what's more, there should be a large number of intermolecular hydrogen bonds between amide groups of the synthesized multiblock copolyamides in the vesicles. Thus, we deduce that the vesicles might be disrupted under an external ultrasound stimulus.

As proof-of-principle experiments, the release behaviour of the MBCPA vesicles encapsulated with nile red (NR) was studied under the ultrasound with the power of 150 W and the frequency of 40 KHz. NR can be solubilized in the hydrophobic interiors of the MBCPA vesicles. When the vesicles were disrupted, the encapsulated NR dyes would be released to water to form aggregates, and a quenching of fluorescence could be detected.[16] So, NR can be used as a probe to detect vesicular disruption based on the change of its emitted fluorescence. Fig. 5a shows that the fluorescence intensity of MBCPA vesicles decreases gradually with increasing the cumulative ultrasonic time. There is almost 50% fluorescence decrease after 14 min's ultrasonic irradiation (Fig. 5b). Since the ultrasonication will increase the solution temperature, the ultrasound was stopped for one minute after 30 seconds of irradiation. In addition, some ice was added to prevent the increase of the solution temperature above 35 ^{o}C. As the control experiments, almost no fluorescence changes were observed for the NR-loaded MBCPA vesicles in room temperature (Fig. S8, ESI†, Curve MBCPA-rt in Fig. 5b) and at 35 ^{o}C (Fig. S8, ESI†, Curve MBCPA-35 ^{o}C in Fig. 5b) in the absence of ultrasonic irradiation. Thus, the large decrease in the fluorescence intensity should be attributed to the release of NR dyes from the MBCPA vesicles, that is, the vesicles should be disrupted by the ultrasound. The disruption of MBCPA vesicles by ultrasound was also proved by the TEM measurement (Fig. S9, ESI†). Moreover, to further reveal the uniqueness of ultrasound-responsive behaviour of MBCPA vesicles, another ultrasound release experiment of NR-loaded hyperbranched polymer (HBPO-star-PEO) vesicles was also performed,[17] where HBPO represents the hydrophobic hyperbranched poly(3-ethyl-3-oxetanemethanol) core and PEO represents the hydrophilic poly(ethylene oxide) arm. From Fig. S8c (ESI†), we can find that there is only 5% fluorescence decrease, after 14 mins' ultrasonication, which indicates that the HBPO-star-PEO vesicles are not ultrasound-responsive.

To our knowledge, the MBCPA vesicles reported here represent a new kind of ultrasound-responsive vesicles. The micro differential scanning calorimetry (micro-DSC) and infrared spectroscopy measurements of MBCPA vesicle aqueous solution at a concentration of 1 mg/mL both indicate that the intermolecular hydrogen bonds inside the MBCPA vesicles are broken after ultrasonic irradiation (Figs. S10 and S11, ESI†). This might be the origin of ultrasound stimuli-responsive behaviour of MBCPA vesicles.

Conclusions

In conclusion, herein we have demonstrated the formation of ultrasound responsive vesicles with an ultrathin membrane through the self-assembly of multiblock copolyamides. The computer simulation results have deepened our understanding on the self-assembly pathway of the vesicles which is consistent with the experimental results, and have also demonstrated that the vesicles possess a combined bilayer and monolayer structure. In addition, the origin of the ultrasonic responsivity has been studied, and it is probably due to the break of intermolecular hydrogen bonds inside the vesicles. We believe that the present work has extended the family of polymer vesicles with new structure and property. Furthermore, we expect that the as-prepared ultrasound responsive vesicles might have some application in controlled drug release, and this work is still in progress.

Acknowledgements

We thank the National Basic Research Program (2013CB834506), China National Funds for Distinguished Young Scholar (21225420), the National Natural Science Foundation of China (91527304, 21474062) and "Shu Guang" project supported by Shanghai Municipal Education commission and Shanghai Education Development Foundation (13SG14) for financial support.

Notes and references

1 (a) A. D. Bangham, M. M. Standish and J. C. Watkins, *J. Mol. Biol.*, 1965, **13**, 238; (b) Y. Y. He, Z. B. Li, P. Simone and T. P. Lodge, *J. Am. Chem. Soc.*, 2006, **128**, 2745; (c) J. H. Fendler, *Acc. Chem. Res.*, 1980, **13**, 7; (d) J. M. Gebicki and M. Hicks, *Nature*, 1973, **243**, 232; (e) L. Zhang and A. Eisenberg, *Science*, 1995, **268**, 1728; (f) J. S. Qian, M. Zhang. L, Manners and M. A. Winnik, *Trends Biotechnol.*, 2010, **28**, 84; (g) B. M. Discher, Y.-Y. Won, D. S. Ege, J. C.-M. Lee, F. S. Bates, D. E. Discher and D. A. Hammer, *Science*, 1999, **284**, 1143; (h) P. L. Luisi, P. Walde and T. Oberholzer, *Curr. Opin. Colloid Interface Sci.*, 1999, **4**, 33; (i) X. Guo and F. C. Szoka Jr., *Acc. Chem. Res.*, 2003, **36**, 335.

2 (a) P. L. Soo and A. Eisenberg, *J. Polym. Sci: Polym.*, 2004, **42**, 923; (b) E. W. Kaler, A. K. Murthy, B. E. Rodriguez and J. A. N. Zasadzinski, *Science*, 1989, **245**, 1371; (c) J. C. M. van Hest, D. A. P. Delnoye, M. W. P. L. Baars, M. H. P. van Genderen and E. W. Meijer, *Science*, 1995, **268**, 1592; (d) E. Blasco, J. Serrano, M. Pinol and L. Oriol, *Macromolecules*, 2013, **15**, 5951; (e) L. H. Wang, X. M. Xu, C. Y. Hong, D. C. Wu, Z. Q. Yu and Y. Z. You, *Chem. Commun.*, 2014, **68**, 9676; (f) W. F. Jiang, Y. F.

Zhou and D. Y. Yan, *Chem. Soc. Rev.*, 2015, **12**, 3874; (g) K. C. Jie, Y. J. Zhou, Y. Yao and F. H. Huang, *Chem. Soc. Rev.*, 2015, **44**, 3568; (h) A. K. A. Silva, R. D. Corato, T. Pellegrino, S. Chat, G. Pugliese, N. Luciani, F. Gazeau and C. Wilhelm, *Nanoscale*, 2013, **5**, 11374; (i) Y. Yu, X. G. Jiang, S. Y. Gong, L. Feng, Y. Q. Zhong and Z. Q. Pang, *Nanoscale*, 2014, **6**, 3250.

3 F. S. Bates, M. A. Hillmyer, T. P. Lodge, C. M. Bates, K. T. Delaney and G. H. Fredrickson, *Science*, 2012, **336**, 434.

4 (a) S. Ludwigs, A. Boker, A. Voronov, N. Rehse, R. Magerle and G. Krausch, *Nat. Mater.*, 2003, **2**, 744; (b) C. Ott. R. Hoogenboom, S. Hoeppener, D. Wouters, J. F. Gohy and U. S. Schubert, *Soft Matter*, 2009, **5**, 84; (c) H. Tan, Z. G. Wang, J. H. Li, Z. C. Pan, M. M. Ding and Q. Fu, *ACS Macro Lett.,* 2013, **2**, 146.

5 J. Zhang, Z. Y. Lu and Z. Y. Sun, *Soft Matter*, 2013, **9**, 1947.

6 (a) N. A. Hadjiantoniou, A. I. Triftaridou, D. Kafouris, M. Gradzielski and G. S. Patrickios, *Macromolecules*, 2009, **42**, 5492; (b) S. Y. Ma, M. Y. Xiao and R. Wang, *Langmuir*, 2013, **29**, 16011; (c) A. Halperin, *Macromolecules*, 1991, **24**, 1418.

7 (a) N. A. J. M. Sommerdijk, S. J. Holder, R. C. Hiorns, R. G. Jones and R. J. M. Nolte, *Macromolecules*, 2000, **33**, 8289; (b) M. M. Ding, J. H. Li, X. He, N. J. Song, H. Tan, Y. Zhang, L. Zhou, Q. Gu, H. Deng and Q. Fu, *Adv. Mater.*, 2012, **24**, 3639; (c) L. Q. Yu, L. J. Zhou, M. M. Ding, J. H. Li, H. Tan, Q. Fu and X. L. He, *J. Colloid Interface Sci.*, 2011, **358**, 376; (d) M. M. Ding, X. L. He, L. J. Zhou, J. H. Li, H. Tan, X. T. Fu and Q. J. Fu, *J. Controlled Release*, 2011, **152**, 87; (e) S. J. Holder, R. C. Hiorns, N. A. J. M. Sommerdijk, S. J. Williams, R. G. Jones and R. J. M. Nolte, *Chem. Commun.*, 1998, 1445.

8 (a) J. Z. Du, Y. Q. Tang, A. L. Lewis and S. P. Armes, *J. Am. Chem. Soc.,* 2005, **127**, 17982; (b) S. H. Qin, Y. Geng, D. E. Discher and S. Yang, *Adv, Mater.*, 2006, **18**, 2905. (c) A. Napoli, M. Valentini, N. Tirelli, M. Muller and J. A. Hubbell, *Nat. Mater.*, 2004, **3**, 183; (d) A. C. Coleman, J. M. Belerle, M. C. Stuart, B. Macia, G. Caroli, J. T. Mika, D. J. van Dijken, J. Chen, W. R. Browne and B. L. Feringa, *Nat. Nanotech.*, 2011, **6**, 547; (e) C. W. Lin, Y. H. Chen and W. S. Chen, *J. Med. Ultras*., 2012, **20**, 87; (f) Q. Yan, J. Yuan, Z. Cai, Y. Xin, Y. Kang and Y. Yin, *J. Am. Chem. Soc.,* 2010, **132**, 9268; (g) A. E. Dunn, D. J. Dunn, A. Macmillan, R. Whan, T. Stait-Gardner, W. S. Price, M. Lim and C. Boyer, *Polym. Chem.*, 2014, **5**, 331; (h) B. Karagoz, J. Yeow, L. Esser, S. M. Prakash, R. P. Kuchel, T. P. Davis and C. Boyer, *Langmuir,* 2014, **30**, 10493; (i) T. T. T. N'Guyen, H. T. T. Duong, J. Basuki, V. Montembault, S. Pascual, C. Guibert, J. Fresnais, C. Boyer, M. R. Whittaker, T. P. Davis and L. Fontaine, *Angew. Chem.,* 2013, **125**, 14402.

9 (a) W. Q. Chen and J. Z. Du, *Sci. Rep-UK.,* 2013, **3**, 1; (b) W. Zhou, F. Meng, G. Engbers and J. Feijen, *J. Controlled Release,* 2006, **116**, e62.

10 (a) N. Yamazaki and F. Higashi, *J Poly Sci Part A: Polym. Chem.*, 1974, **12**, 185; (b) C. Ruijer, W. F. Jager, J. Groenewold and S. J. Picken, *Macromolecules*, 2006, **39**, 3826.

11 (a) J. R. Howse, R. A. L. Jones, G. Battaglia, R. E. Ducker, G. L. Leggett and A. J. Ryan, *Nat. Mater.,* 2009, **8**, 507; (b) J. Wang, Y. Z. Ni, W. F. Jiang, H. M. Li, Y. N. Liu, S. L. Lin and Y. F. Zhou, *small*, 2015, **11**, 4485.

12 (a) Y. Y. Han, H. Z. Yu, H. B. Du and W. Jiang, *J. Am. Chem. Soc.,* 2010, **132**, 1144; (b) X. H. He and F. Schmid, *Phys. Rev. Lett.,* 2008, **100**, 137802.

13 (a) V. Percec, D. A. Wilson, P. Leowanawat, C. J. Wilson, A. D. Hughes, M. S. Kaucher, D. A. Hammer, D. H. Levine, A. J. Kim, F. S. Bates, K. P. Davis, T. P. Lodge, M. L. Klein, R. H. DeVane, E. Aqad, B. M. Rosen, A. O. Argintaru, M. J. Sienkowska, K. Rissanen, S. Nummelin and J. Ropponen, *Science*, 2010, **328**, 1009; (b) Y. Liu, C. Y. Yu, H. B. Jin, B. B. Jiang, X. Y. Zhu, Y. F. Zhou, Z. Y. Lu and D. Y. Yan, *J. Am. Chem. Soc.*, 2013, **135**, 4765.

14 (a) D. E. Discher and A. Eisenberg, *Science,* 2002, **297**, 967; (b) M. Antonietti and S. Forster, *Adv. Mater.*, 2003, **15**, 1323; (c) A. Blanazs, S. P. Armes and A. J. Ryan, *Macromol. Rapid Commun.*, 2009, **30**, 267.

15 (a) J. Rodriguez-Hernandez and S. Lecommandoux, *J. Am. Chem. Soc.*, 2005, **127**, 2026; (b) Y. Barenholz, *Curr. Opin. Colloid Interface Sci.*, 2001, **6**, 66; (c) T. Lian and R. J. Y. Ho, *J. Pharm. Sci.,* 2001, **90**, 667.

16 (a) A. P. Goodwin, J. L. Mynar, Y. Ma, G. R. Fleming and J. M. J. Frechet, *J. Am. Chem. Soc.*, 2005, **127**, 9952; (b) J. Xuan, M. Pelletier, H. S. Xia and Y. Zhao, *Macromol. Chem. Phys.*, 2011, **212**, 498.

17 Y. F. Zhou and D. Y. Yan, *Angew. Chem. Int. Ed.*, 2004, **43**, 4896.

A novel ultrasound-responsive polymer vesicles with ultrathin wall and special packing model were generated from an amphiphilic multiblock copolyamide.

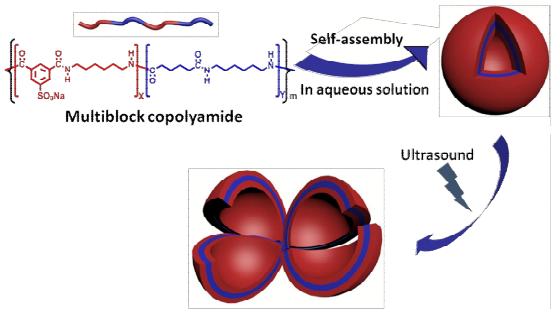

Supporting Information

Ultrasound-responsive ultrathin multiblock copolyamide vesicles

Lei Huang,[a] Chunyang Yu,[b] Tong Huang,[b] Shuting Xu,[b] Yongping Bai,[a] Yongfeng Zhou[b*]*

[a]*School of Chemical Engineering and Technology, Harbin Institute of Technology, Harbin 150001, P.R. China. Email: baifengbai@hit.edu.cn*

[b]*School of Chemistry and Chemical Engineering, State Key Laboratory of Metal Matrix Composite, Shanghai Jiao Tong University, Shanghai 200240, China. Fax: (+86) 21 54741297; Email: yfzhou@sjtu.edu.cn*

1. Materials.

N-methyl-2-pyrrolidone (NMP, Shanghai Chemical Reagent Co., >99%) was refluxed with sodium and distilled to remove the water before use. Triphenyl phosphite (TPP, TCI, >97%) was purified by vacuum-distillation before use. Anhydrous calcium chloride was dried under vacuum at 180^{o}C for 24h. Pyridine (Py, Shanghai Chemical Reagent Co., >99%), acetic acid, hexamethylenediamine (HMD), hexanedioic acid (HA), methanol (MeOH, Shanghai Chemical Reagent Co., >99%) nile red (NR, TCI, >99%) were used as received. Sodium 5-sulfoisophthalate (NaSIPA, TCI) and anhydrous ethanol (Acros) were also used as received.

2. Instruments and Measurements

Fourier Transform Infrared Spectroscopy (FTIR)

FTIR and liquid IR measurements were carried out on a Perkin-Elmer Spectrum 100 PC Fourier transform infrared spectrometer in the range of 500~4500 cm^{-1} with an accuracy of 4 cm^{-1}. For liquid infrared spectra, first, a droplet of multiblock copolyamide vesicles aqueous solution (1mg/mL) was sprayed onto the calcium fluoride wafer at room temperature, and then another calcium fluoride wafer was used as a cover to encapsulate the MBCPA vesicles solution.

Nuclear Magnetic Resonance (NMR) and Intrinsic viscosity

The Varian Mercury Plus spectrometer was used to obtain ^{1}H NMR spectra (400 MHz) with sulfuric acid (D_2SO_4-d_2) used as solvent. Intrinsic viscosity in sulfuric acid (96%) was determined in an Ubbelohde viscometer at 30 $\pm$0.1 ^{o}C.

Thermal Gravity Analysis (TGA)

The thermogravimetric analysis (TGA) was performed on a Perkin-Elmer Q5000IR thermobalance with heating rate of 20 ^{o}C min^{-1} and nitrogen was used as the purge gas.

Transmission Electron Microscopy (TEM)

Transmission Electron Microscopy (TEM) analysis was performed on a JEM-2100/INCA OXFORD instrument operating at an accelerating voltage of 200 KV. The samples were sprayed onto the carbon-coated copper grids and air-dried at room temperature before measurement. The stained TEM sample was prepared by adding 1-3 drops of 3% phosphotungstic acid aqueous into the assembly solution (0.1mg/mL). Then, the stained solution was dropped onto the carbon-coated copper grids, and the grids were dried at room temperature for 24 h.

Dynamic light scattering (DLS)

The dynamic light scattering (DLS) measurement was performed in aqueous solution at 25 ^{o}C at a scattering angle of 90 °, using a Malvern Zetasizer Nano S apparatus equipped with a 4.0 mW laser operating at λ=633 nm.

Atomic Force Microscopy (AFM)

AFM measurements were carried out on a multimode Nanoscope-IIIa Scanning Probe Microscope equipped with a MikroMasch silicon cantilever, NSCII (radius < 10nm, resonance frequency = 300 kHz, spring constant = 40 N/m) with tapping mode (TM) at room temperature. The sample for AFM observations were prepared by depositing several drops of the solution (1 mg/mL) onto the surface of fresh cleaved mica, and the samples were air-dried at room temperature.

Fluorescence spectrophotometer (FL)

For the fluorescence spectra of the vesicles loaded with NR, a fluorescence spectrophotometer (LS 50B, Perkin Elmer, Inc, USA) was used, with the excitation wavelength set at 600 nm. The concentration of the vesicle solution is 1 mg/mL.

Micro-Differential Scanning Calorimetry (micro-DSC)

Micro-DSC measurements were carried out on a VP DSC from MicroCal. The volume of the sample cell is 0.509 mL. The reference cell was filled with deionized water. The sample solution with a concentration of 1.0 mg/mL was degassed at 25 ^{o}C for half an hour and equilibrated at 10 ^{o}C for 1h before the heating process with the heating rate of 1.0 ^{o}C/min.

3. Synthesis and Characterization of MBCPAs

The multiblock copolyamide, MBCPA (feed ratio: 0.4:1), was synthesized by solution polycondensation in two steps following the reaction method described by Yamazaki.[1-4] As show in Fig. S1, PASIP and PA66 segments were synthesized in the first step, respectively; in the second step, the multiblock copolyamide was synthesized by coupling of these two segments.

In a typical preparation of PA6SIP segments, a three neck 100mL round bottom flask equipped with mechanical stirrer and nitrogen inlet was charged with PA6SIP salts and $CaCl_2$ (18%, w/w), 7.1 mL of NMP, 1 mL of pyridine and 1.1 mL of triphenyl phosphite. Then, this reaction mixture was heated to 100^{o}C for 3 h under N_2 atmosphere. The preparation of PA66 segments was prepared by the similar procedure.

Then, the solution of PA6SIP segment was transferred quickly to the reaction vessel of PA66 segment. An additional amount of $CaCl_2$ anhydrous (0.05 g) was added in the new reaction system. The reaction was continued for another 22 h at 100 ^{o}C under N_2 atmosphere. Finally, the copolymer solution was precipitated in 250mL of methanol. The fibrous product obtained was collected by filtration and then washed several times with methanol. The copolyamide as obtained was dried in a vacuum oven at 100 ^{o}C for 24 h. For simplicity, we denoted it as MBCPA.

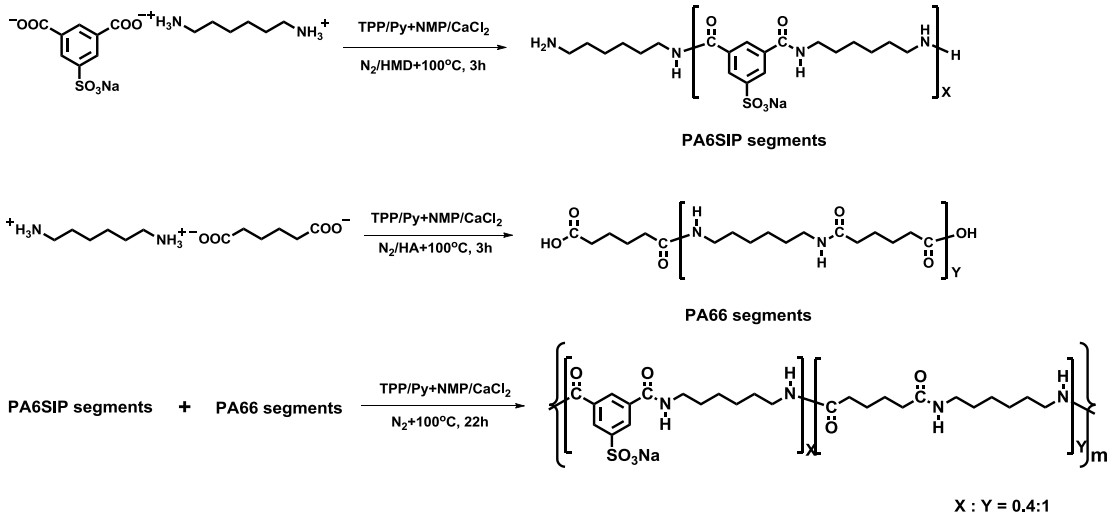

Fig. S1 The synthesis scheme of the multiblock copolyamide.

Then, viscosimetry in concentrated (96 wt %) sulfuric acid was performed in order to determine the intrinsic viscosities $[\eta]$ of the multiblock copolyamide. Then, according to the following semiempirical equation induced by Ruijter and Picken et al., the viscosity average molecular weight for the multiblock copolyamide can be estimated.

$$M_{\mathrm{AB}}^{3/2}[\eta]_{\mathrm{copolymer}} = M_{\mathrm{v,copolymer}}^{1/2}((M_A[\eta]_{\mathrm{A}})^{2/3} + (M_{\mathrm{B}}[\eta]_{\mathrm{B}})^{2/3})^{3/2}$$

Fig. S2 The semiempirical equation of viscosity average molecular weight of the multiblock copolyamide.

Where M_{AB} is the mass of the repeating unit in the block copolyamide. In addition, M_A and M_B represent the molar masses and $[\eta]_A$ and $[\eta]_B$ the corresponding intrinsic viscosities of respectively the PA66 and PA6SIP blocks.

FTIR were used to ascertain the structure of as-prepared MBCPA. Fig. S3 displays the typical FTIR spectra of the product, which exhibit the characteristic bands associated with polyamides. Bands with maximums at 3305 cm^{-1} (hydrogen-bonded N-H stretching), round 1642 cm^{-1} (C=O stretching), and round 1540 cm^{-1} (C-N stretching and CO-N-H bending) all correspond to motions associated with the amide group. Meanwhile, the absorption bands at round 1043 cm^{-1} (O=S=O symmetric stretching) are attributed to the sulfonate groups. The results above should prove the formation of copolyamide.

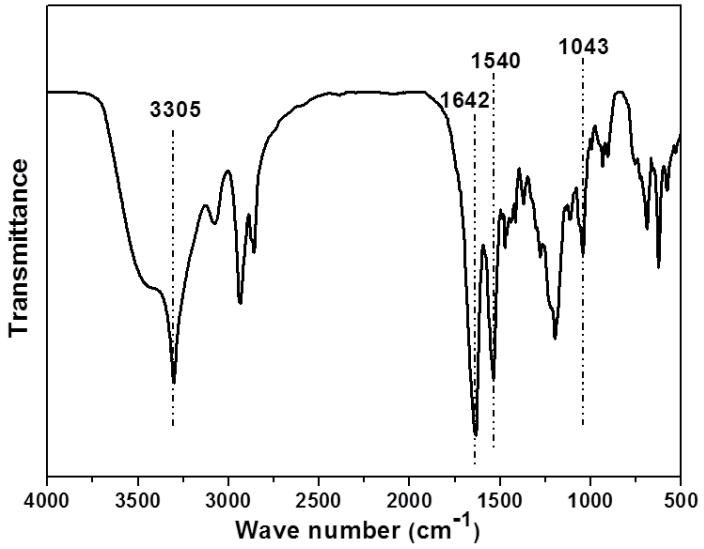

Fig. S3 The FTIR spectrum of as-prepared MBCPAs.

4. The DSC measurements of MBCPAs

For further demonstrate the multiblock structure of MBCPA, DSC was used to prove that the prepared MBCPA was the multiblock copolyamide rather than the physical blend of PA66 and PA6SIP. It is well known that there is bigger phase separation in the physical blend of PA66 and PA6SIP than the prepared copolyamide MBCPA. Hence, the physical blend of PA66 and PA6SIP might show two melting peak. However, the MBCPA should display only one peak in DSC measurement when the two blocks are not adequate long. Fig. S4 shows a typical DSC curves of MBCPAs and the physical blend (mass ratio PA6SIP : PA66 = 0.46 : 1). The blend displays two melting peaks around 230 ^{o}C and 258 ^{o}C, respectively. Otherwise, the MBCPA possess only one melting point of 252 ^{o}C. These results indicate that the prepared MBCPA is not the physical blend of PA66 and PA6SIP.

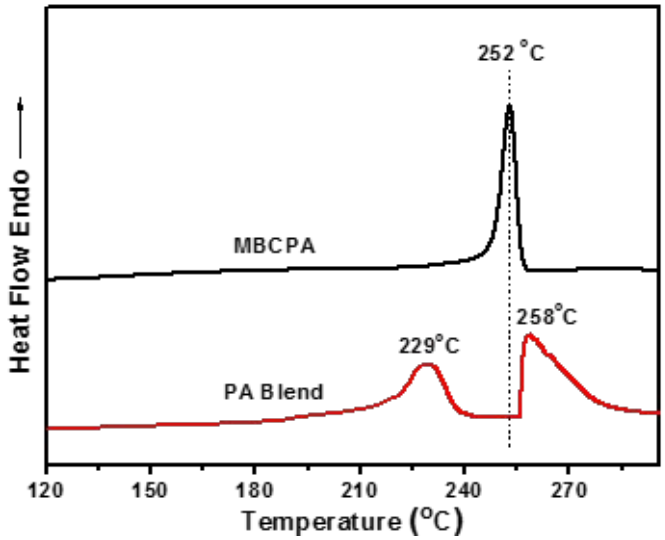

Fig. S4 The DSC curves of as-prepared MBCPAs and the physical blend of PA66 and PA6SIP.

5. The TEM image of MBCPA vesicles

TEM was used to characterize the morphology of the self-assemblies from MBCPAs. Most of the self-assemblies are spherical and closed particles. Fig. S5 shows some special particles with holes on the surface (white arrows), which indicates the self-assemblies are hollow in nature. The hole on the vesicle was probably generated by the disruption of vesicles due to the evaporation of water during the sampling process for TEM measurement.

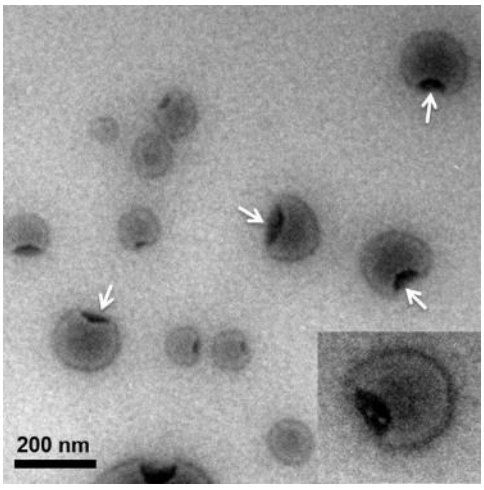

Fig. S5 The TEM image of the MBCPA self-assemblies with holes.

6. Characterizations of the vesicular structure

TEM was used to characterize the morphology of the self-assemblies from the multiblock copolyamide. Fig. S6 displays a typical TEM image of the intermediates of vesicles. From Fig. S6, some lamellar structures, the intermediates of MBCPA vesicles with two or more holes and vesicles with closed holes could be observed, which supports the self-assembly pathway of the vesicles (Fig. 3) as disclosed by the DPD simulations very well.

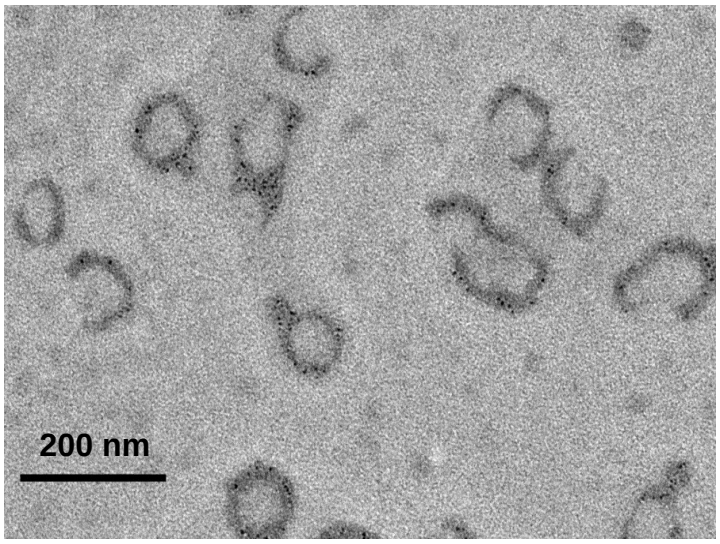

Fig. S6 The TEM image of the self-assembled intermediates for MBCPA vesicles.

7. Coarse-grained MBCPA model and DPD simulation method

Dissipative particle dynamics (DPD) is a particle-based, mesoscale simulation technique. First introduced by Hoogerbrugge and Koelman in 1992[8] and improved by Español and Warren,[9] DPD method takes some of the merit of molecular dynamics (MD) and allows the simulation of hydrodynamic behavior of large complex fluid systems up to the microsecond range.

A. Interactions between DPD Beads. In general, a DPD bead represents a group of atoms, and all of the beads in the system are assumed to possess the same volume. The force on bead *i* is given by the sum of a conservative force $\vec{F}_{ij}^{C}$, a dissipative force $\vec{F}_{ij}^{D}$, and a random force $\vec{F}_{ij}^{R}$:

$$\vec{F}_i = \sum_{j \neq i} (\vec{F}_{ij}^{C} + \vec{F}_{ij}^{D} + \vec{F}_{ij}^{R}) \qquad \text{(Equation 1)}$$

The sum runs over all other beads within a certain cutoff radius R_c. Different parts of the forces are given by:

$$\vec{F}_{ij}^{C} = -\alpha_{ij}\omega^{C}(r_{ij})\vec{e}_{ij} \quad , \qquad \text{(Equation 2)}$$

$$\vec{F}_{ij}^{D} = -\gamma\omega^{D}(r_{ij})(\vec{v}_{ij}\cdot\vec{e}_{ij})\vec{e}_{ij} \quad , \qquad \text{(Equation 3)}$$

$$\vec{F}_{ij}^{R} = \sigma\omega^{R}(r_{ij})\xi_{ij}\Delta t^{-1/2}\vec{e}_{ij} \quad , \qquad \text{(Equation 4)}$$

where $\vec{r}_{ij} = \vec{r}_i - \vec{r}_j$, $r_{ij} = |\vec{r}_{ij}|$, $\vec{e}_{ij} = \vec{r}_{ij}/r_{ij}$, $\vec{r}_i$ and $\vec{r}_j$ are the positions of bead *i* and bead *j*, respectively. $\vec{v}_{ij} = \vec{v}_i - \vec{v}_j$, $\vec{v}_i$ and $\vec{v}_j$ are the velocities of bead *i* and bead *j*, respectively. α_{ij} is a constant that describes the maximum repulsion between interacting beads. γ and σ are the amplitudes of dissipative and random forces, respectively. ω^C, ω^D and ω^R are three weight functions for the conservative, dissipative, and random forces, respectively. For the conservative force, we choose $\omega_{ij}^{C}(r_{ij})=1-r_{ij}/R_c$ for $r_{ij}<R_c$ and $\omega_{ij}^{C}(r_{ij})=0$ for $r_{ij}\geq R_c$. $\omega_{ij}^{D}(r_{ij})$ and $\omega_{ij}^{R}(r_{ij})$ follow a certain relation according to the fluctuation-dissipation theorem, i.e., $\omega_{ij}^{D}(r)=[\omega_{ij}^{R}(r)]^2$, and $\sigma^2=2\gamma k_BT$, so that the system has a canonical equilibrium distribution. According to Groot and Warren,[3] we choose a simple form of ω^D and ω^R as following:

$$\omega^{D}(r) = \begin{cases} (1-r/R_c)^2 & (r < R_c) \\ 0 & (r \geq R_c) \end{cases} \quad . \qquad \text{(Equation 5)}$$

ξ_{ij} in Equation 4 is a random number with zero mean and unit variance, chosen independently for each interacting pair of beads at each time step Δt. A modified version of velocity-Verlet algorithm is used here to integrate the equations of motion. For simplicity, the cutoff radius R_c, the bead mass *m*, and the temperature k_BT are taken as the units of the simulations, i.e., $R_c=m=k_BT=1$; thus the time unit $\tau=(mR_c^2/k_BT)^{1/2}=1$.

Moreover, in our DPD simulations, a harmonic spring force $\vec{F}_{ij}^{S} = -C^{S}(r_{ij} - r_{eq}^{S})\vec{e}_{ij}$ ($C^S = 4$, $r_{eq}^S = 0$) was adopted between bonded beads *i* and *j* in the polymer. Note that $\vec{F}^S$ is used to impose connection between beads of a polymer, and the choice of *C* and r_0 will not affect the statistical behavior of the system.

B. System Parameters. In this study, we consider a typical DPD model of $[(AB)_2(CB)_5]_n$ (n=3) to represent a multiblock copolyamide (Fig. S7), where "A" represents the hydrophilic benzene sulfonic acid sodium salt repeat unit, "B" represents the hydrophobic hexamethylenediamine repeat unit, "C" represents the

hydrophobic hexanedioic acid repeat unit. Meanwhile, we use "S" represents the solvent particle.

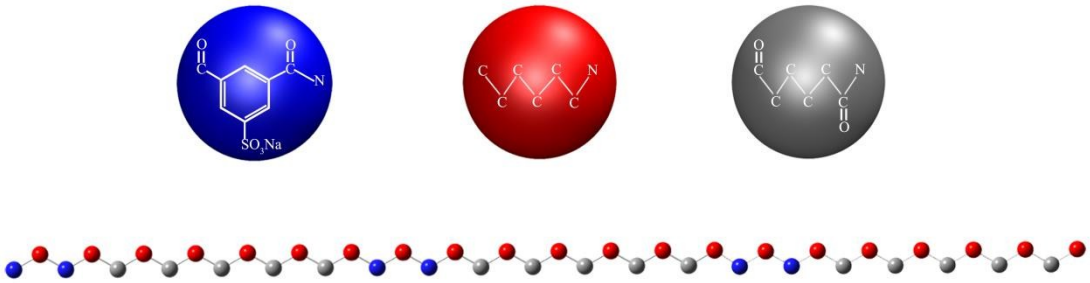

Fig. S7 The coarse-grained models for $[(AB)_2(CB)_5]_n$ (n=3) structure. Blue: A type bead (benzene sulfonic acid sodium salt block); red: B type bead (hexamethylenediamine block); gray: C type bead (hexanedioic acid block).

Generally, the DPD interaction parameters (α_{ij}) can be estimated based on the relationship between α and the Flory-Huggins parameters χ established by Groot and Warren,[7]

$$\alpha_{ij} = \alpha_{ii} + 3.27\chi_{ij}, \quad \text{(Equation 6)}$$

where α_{ii}=25 is for the same type of bead. To calculate the Flory-Huggins parameters, all-atom molecular dynamics (AAMD) simulation was performed for pure and binary components as listed in Table S1. Here, all the AAMD simulations were carried out by using GROMACS[8] software package to estimate χ parameters between different components. In the AAMD simulations, the systems of A, B, C, water, A/B, A/C, B/C, A/water, B/water and C/water were firstly constructed in a simulation box with 3D periodic boundary conditions, respectively. At the beginning of all the simulations, energy minimizations were performed to relax the unfavorable local structures of the molecules. Subsequently, 5 ns MD simulations were performed using General Amber force field[9] in NPT ensemble with v-rescale[10] thermostat and Parrinello-Rahman barostat,[11] and the velocity Verlet integrator was used for integrating the equations of motion. The TIP4P water model is used to calculate interaction parameter between polymer segment and water. A time step of 1fs was employed, and all bonds to hydrogen were constrained by using LINCS algorithm. The cutoff radius of 10 Å with the nearest image convention was used for the van der Waals interaction calculations. The electrostatic interactions were evaluated by particle mesh Ewald (PME) method with a direct space cutoff distance of 10 Å. All calculations were performed at a

pressure P = 1.0 atm and temperature T = 303.0 K. The last 1.0 ns trajectory was used to calculate potential energy.

For binary components i and j, the Flory-Huggins parameter χ_{ij} can be estimated by the following equation:

$$\chi_{ij} = \frac{\Delta E_{mix} V_{bead}}{k_B T}, \quad \text{(Equation 7)}$$

where V_{bead} is the average volume of the coarse-grained bead in our DPD simulations, it was calculated by the following equation:

$$V_{bead} = \frac{V_a \times N_a + V_b \times N_b + V_c \times N_c}{N_a + N_b + N_c} = \frac{264*6+217*21+198*15}{42} = 217\text{Å}^3 \approx 7V_{water}; \quad \text{(Equation 8)}$$

k_b is boltzmann constant and T is temperature; ΔE_{mix} is the mixing energy

$$\Delta E_{mix} = \varphi_i \left(\frac{E_{coh}}{V}\right)_i + \varphi_j \left(\frac{E_{coh}}{V}\right)_j + \varphi_{ij} \left(\frac{E_{coh}}{V}\right)_{ij} \quad \text{(Equation 9)}$$

Here, φ_i and φ_j are the volume fractions of the components i and j. The cohesive energy E_{coh} can be obtained by

$$E_{coh} = \sum_{i=1}^{n} E_{nb}^{isolated} - E_{nb}^{n}, \quad \text{(Equation 10)}$$

where $E_{nb}^{isolated}$ is the non-bonded energy for the ith isolated A or B or C segments in vacuum, and E_{nb}^{n} is the non-bonded energy of the model with nA or nB or nC in the simulation box. In the meanwhile, the solubility parameter δ of each pure components can be obtained by the square root of the cohesive energy density,

$$\delta = \sqrt[2]{E_{coh}/V}, \quad \text{(Equation 11)}$$

where V is the volume of the simulation box. Then, according to Equation 9, the DPD interaction parameters α_{ij} were calculated from the Flory-Huggins χ parameters and shown in Table S2

Table S1. Pure and binary components examined by MD simulations.

Components	Number of molecules	Density (g/cm^3)	Volume ($Å^3$)	$\delta(J/cm^3)^{1/2}$	χ
H_2O	5066	0.991	30	47.59	-
A	100	1.581	264	46.06	-
B	100	0.773	217	20.34	-
C	100	1.084	198	29.30	-
A/B	100/100	1.116	-	-	12.62
A/C	100/100	1.029	-	-	15.56
B/C	100/100	0.927	-	-	1.11
A/H_2O	50/4000	1.076	-	-	-0.21
B/H_2O	50/4000	0.974	-	-	10.44
C/H_2O	50/4000	0.997	-	-	8.64

Table S2. Conservative force constants α_{ij} used by DPD simulations.

	H_2O	A	B	C
H_2O	25			
A	24.31	25		
B	59.14	66.27	25	
C	53.25	75.88	28.63	25

For easy numerical handling, we used reduced units in DPD simulations. However, we could convert them to the real units by mapping the bead size and the diffusion coefficient. Since the average volume of one bead in DPD simulations is about 210 Å^3 and the reduced number density is 3, a cube of size R_c^3, therefore, corresponds to 630 Å^3. Thus, the length scale in the simulations can be obtained as $R_c = \sqrt[3]{630\text{Å}^3} = 8.57\text{Å}$. Moreover, Groot[12] showed that the effective time unit τ of the DPD simulation can be obtained by matching the bead diffusion coefficient in the simulation to that of pure water. According to the analysis at α_{ii}=25 and ρ=3, the relationship between the effective time unit τ and N_m can be expressed as:

$$\tau = \frac{N_m D_{sim} R_c^2}{D_{water}} = 25.7 \pm 0.1 N_m^{5/3} \text{ [ps]} \quad \text{(Equation 12)}$$

In Equation 12, N_m is the number of water molecules that each DPD bead represents, which equals 7 in our simulations. Therefore in our DPD simulations, the effective time unit τ is 658 ps and the integration time step Δt = 13.2 ps.

All the DPD simulations were performed in a cubic box of size 60×60×60 R_c^3 containing 6.48×10^5 CG beads by using HOOMD package[13-15] on NVIDIA Tesla K20 GPU. The concentration of the block copolymers is 0.06. Periodic boundary conditions were applied.

In addition, we define the radial density distribution $\rho(r)$ as the average number density of each type particles at a radial distance r from the center of mass of the vesicle to the outside of the vesicle. Hence, the integration over r yields the total number of each type particles. The mathematical expression is as $N(r) = 4\pi \int_0^{+\infty} r^2 \rho(r) dr$. However, considering the number density of current DPD simulation is 3, all RDFs are divided by the normalization.

8. The dye release experiments of NR-loaded MBCPA vesicles without ultrasonic irradiation

Fig. S8 shows the fluorescence curves of NR-loaded MBCPA vesicles aqueous solutions at room temperature, 35 ^{o}C and NR-loaded HBPO-star-PEO vesicles aqueous solution, respectively. The NR-loaded MBCPA vesicles aqueous solutions were maintained at room temperature and 35 ^{o}C for 14 min, and it can be seen that their fluorescence intensities have seldom changed. The results indicate that the NR dyes can not been released to water, that is, the MBCPA vesicles have not been disrupted. Moreover, from Fig. S8c, we can also find that the fluorescence intensity of NR-loaded HBPO-star-PEO vesicles have decreased very slightly after 14 min's ultrasonication. There is only 5% fluorescence decrease, that is, the HBPO-star-PEO vesicles have barely been disrupted and they are not ultrasound-responsive.

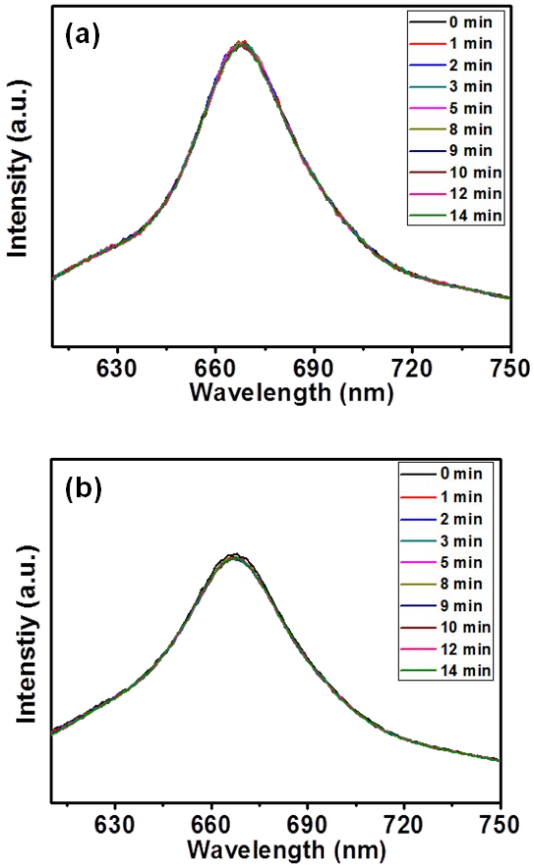

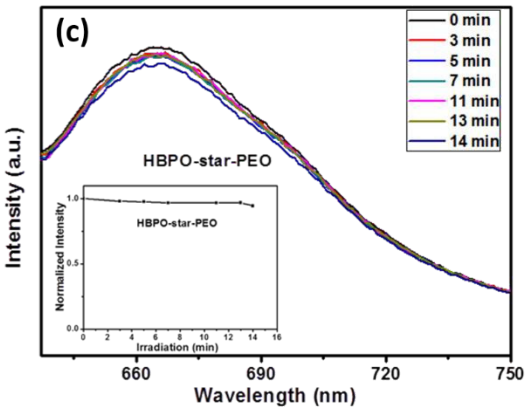

Fig. S8 The fluorescence emission spectra of NR-loaded MBCPA vesicle aqueous solution at the room temperature (a) and at 35^{o}C (b) without untrasonication, and of NR-loaded HBPO-star-PEO vesicle aqueous solution under ultrasonic irradication (c). The inset in image (c) shows the accumulative release of NRs from NR-loaded HBPO-star-PEO vesicles with ultrasound treatment.

9. The effect of ultrasound on the morphologies of MBCPA vesicles

Fig. S9 displays the effect of ultrasound irradiation on the morphologies of the MBCPA vesicles. The MBCPA vesicles transformed into lots of vesicles fragments after ultrasound treatment for 14 min, which indicates that the vesicles should be disrupted by ultrasound.

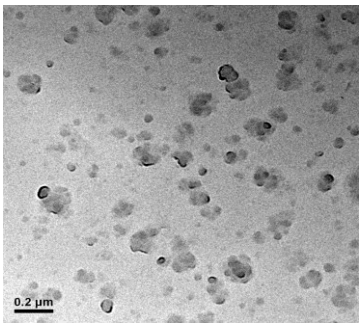

Fig. S9 The TEM image of MBCPA vesicles after ultrasonication treatment for 14 min.

10. The origin of ultrasound-responsive behavior of MBCPA vesicles

To get insight into the nature of ultrasound stimuli-responsive behavior of MBCPA vesicles, the micro-DSC of MBCPA vesicles aqueous solution before and after their ultrasound treatment were investigated. According to Fig. S10, it is clearly noted that the MBCPA vesicle aqueous solution before ultrasound treatment displays one endothermic peak with the onset temperature of 82^{o}C. It is believed that the endothermic peak is attributed to the breakup of intermolecular hydrogen bonds among the multiblock copolyamides in the vesicles. As a contrast, after ultrasonic treatment for 10 min, the endothermic peak of the MBCPA vesicle aqueous solution totally disappeared. In other words, the intermolecular hydrogen bonds in the vesicles might be disrupted due to ultrasonic irradiation.

To further ascertain our speculation, the infrared spectra of MBCPA vesicles aqueous solution before and after their ultrasound treatment were studied. Fig. S11 represent the FTIR spectra obtained in the frequency range of 3000-850 cm^{-1}. From Fig. S11a, it is noted that the intensity of the band (C-N stretching and CO-N-H bending) at round 1539 cm^{-1} decreased after ultrasonic treatment. The decrease of this characteristic band of amide group is directly associated with the decrease of the average strength of the intermolecular hydrogen bond.[5] In addition, the peak position of the band at about 907 cm^{-1} arising from the stretching vibration of C-CO was found to shift to lower frequency, implying that the weakening of intermolecular hydrogen bond. What's more, as shown in Fig. S11b, the absorption bands at round 1475 cm^{-1} and 1416 cm^{-1} are attributed to the shear vibration of the methylene groups adjacent to the amide groups. Obviously, their strengths decreased after ultrasound treatment. These two bands are affected by the intensity of hydrogen bond too. Moreover, similar changes are observed from peaks at 1278 cm^{-1} and 1199 cm^{-1}, which are originated from the coupling of the in-plane vibration of CO-NH and the out-of-plane vibration of methylene and the bending vibration of methylene, respectively.[6,7] It is clear that their intensities both decreased after ultrasound experiment, proving that the intensity of hydrogen bond becomes weaker. As a consequence, it can be believed that the intermolecular hydrogen bonds of MBCPA vesicular assemblies should be

broken after ultrasound experiment. This is the origin of ultrasound stimuli-response behavior of MBCPA vesicles.

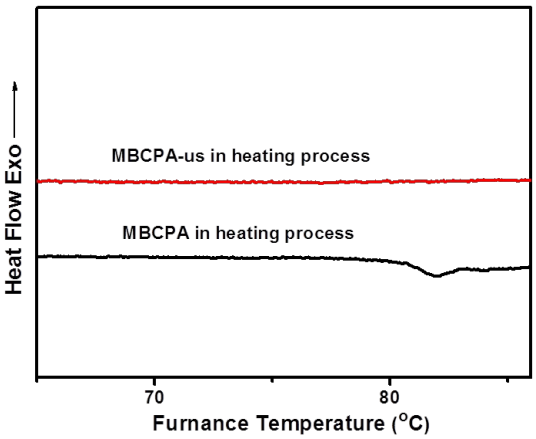

Fig. S10 The micro-DSC curves of MBCPA vesicle aqueous solution before and after ultrasound treatment.

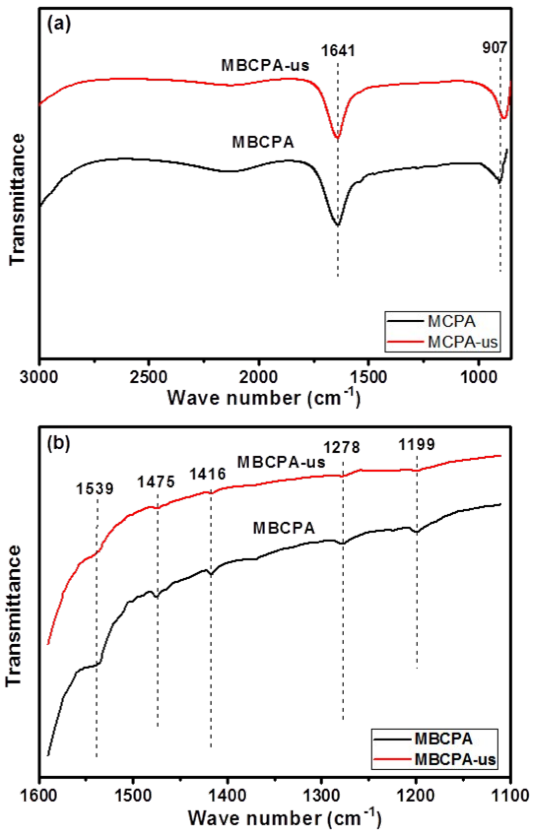

Fig. S11 The liquid infrared spectra of MBCPA vesicle aqueous solution before and after ultrasound treatment.

References

[1] Yang C. P. and Cherng J. J., *J Polym Sci Part A* 1995, **33**, 2209.

[2] Higashi F, Akiyama N. and Ogata SI. *J Polym Sci Part A: Polym Chem* 1983, **21**, 913.

[3] Yamazaki, N. and Higashi F., *J Polym Sci Part A: Polym Chem* 1974, **12**, 185.

[4] Yang, C. P. and Yang, H. W., Chen RS. *J Appl Polym Sci* 2000, **77**, 116.

[5] Hoogerbrugge, P. J. and Koelman, J. M. V. A. *Europhys. Lett.*, 1992, **19**, 155.

[6] Español, P. and Warren, P. *Europhys. Lett.* 1995, **30**, 191.

[7] Groot, R. D. and Warren, P. B. *J. Chem. Phys*. 1997, **107**, 4423.

[8] D. van der Spoel, E. Lindahl, B. Hess, A. R. van Buuren, E. Apol, P. J. Meulenhoff, D. P. Tieleman, A. L. T. M. Sijbers, K. A. Feenstra, R. van Drunen and H. J. C. Berendsen, Gromacs User Manual version 4.5.4, www.gromacs.org (2010).

[9] Wang, J., Wolf, R. M., Caldwell, J. W.,Kollman, P. A. and Case, D. A., *J. Comput. Chem.* 2004, **25**, 1157.

[10] Bussi, G., Donadio, D. and Parrinello, M., *J. Chem. Phys.* 2007, **126**, 014101.

[11] Parrinello, M. and Rahman, A. *J. Appl. Phys.* 1981, **52**, 7182.

[12] Groot, R. D., *J. Chem. Phys.* 2003, **118,** 11265.

[13] HOOMD-blue web page: http://codeblue.umich.edu/hoomd-blue

[14] Anderson, J. A.; Lorenz, C. D.; Travesset, A., *J. Comput. Phys*. 2008, **227**, 5342.

[15] Phillips, C. L.; Anderson, J. A.; Glotzer, S. C., J. Comput. Phys. 2011, **230**, 7191.

[16] Cui, X. W. and Yan, D. Y., *Eur. Polym. J.*, 2001, **39**, 868.

[17] Skrovanek, D. J., Painter, P. C. and Coleman, M. M., *Macromolecules*, 1986, **19**, 699.

[18] Yoshioka, Y., Kohji, T. and Ramesh, C., *Polymer*, 2003, **44**, 6411.

Journal Name

COMMUNICATION

Ultrasound-responsive ultrathin multiblock copolyamide vesicles

Lei Huang,[a] Chunyang Yu,[b] Tong Huang,[b] Shuting Xu,[b] Yongping Bai,[a*] and Yongfeng Zhou[b*]

Received 00th January 20xx,
Accepted 00th January 20xx

DOI: 10.1039/x0xx00000x

www.rsc.org/

This study reports the self-assembly of a novel polymer vesicles from an amphiphilic multiblock copolyamide, and the vesicles have shown a special structure of ultrathin wall thickness of about 4.5 nm and of a combined bilayer and monolayer packing model. Most interestingly, the vesicles are ultrasound-responsive and can release the encapsulated model drugs in response to ultrasonic irradiation.

Among all fantastic supramolecular self-assemblies, vesicles including lipid vesicles (liposomes), surfactant vesicles and polymer vesicles (polymersomes) have drawn great attention due to their great importance in living systems and various applications such as in pharmaceutical, diagnostic, and cosmetic agents.[1] Up to now, polymer vesicles have been obtained from the self-assembly of many kinds of polymer architectures like diblock copolymers, triblock copolymers, star copolymers, graft copolymers, dendrimers and hyperbranched polymers, and have demonstrated great potentials from both the scientific and industrial communities.[2] Herein, we report for the first time on a novel polymer vesicles self-assembled from multiblock copolymers.

As we know, multiblock copolymers are a kind of linear polymers consisting of more than three polymer blocks.[3] Thus, in principle, such a kind of polymer structure can not only enlarge the structural diversity of polymers but also allow the incorporation of more functionalities in one polymer chain.[4] In addition, from the self-assembly aspect, multiblock copolymers can introduce multiple hydrophilic and hydrophobic segments in the polymer chains, which will induce more complex chain folding and phase separation processes when compared with those of diblock or triblock copolymers and then may generate more complicated supramolecular structures. It has been even considered as a simple model for protein folding and DNA packing.[5] However, despite of these advantages, the studies on

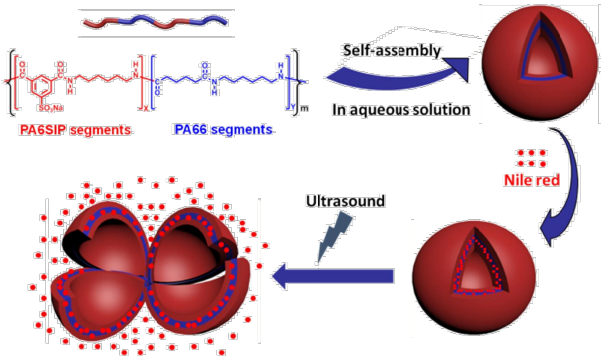

Scheme 1 Synthesis and self-assembly of multiblock copolyamides into ultrasound-responsive vesicles.

the synthesis and self-assembly of multiblock copolymers are still great limited. Among them, Halperin, Wang and Lu et al.[5,6] have performed the computer simulations, while Tan and Sommerdijk et al[7] have conducted the experimental studies. Nevertheless, the obtained self-assemblies are generally limited to micelles.

Herein, as a new progress, we report the self-assembly of vesicles from a multiblock copolyamide (MBCPA, Scheme 1) in water. The obtained vesicles have an ultrathin wall of 4.5 nm. Most interestingly, they can be disrupted and release the encapsulated hydrophobic nile red in response to ultrasonic irradiation. Compared to other stimuli such as pH, oxidation/reduction, temperature, light, alternated magnetic field and electrical field etc., noninvasive ultrasound may possess some unique advantages such as penetrating deeply in the body, relatively easy dynamic examination, providing high resolution images of the soft tissues, easily accessible and low cost etc.[8] Up to now, only few works have been reported on the ultrasound-responsive polymer vesicles generating from the self-assembly of poly(ethylene oxide)-block-poly[2-(diethylamino) ethyl methacrylate- statistical-2-tetrahydrofuranyloxy ethyl methacrylate] (PEO-b- P(DEA-stat-TMA)) and poly (ethylene glycol)-polyactide (PEG-b- PDLLA),[9] and thus the present work represents a new type of the ultrasound-responsive polymer vesicles.

The MBCPAs used here were synthesized by solution polycondensation in two steps following the reaction method

[a] School of Chemical Engineering and Technology, Harbin Institute of Technology, Harbin 150001, PR China. Email: baifengbai@hit.edu.cn
[b] School of Chemistry and Chemical Engineering, State Key Laboratory of Metal Matrix Composites, Shanghai Jiao Tong University, 800 Dongchuan Road, Shanghai 200240, China. Fax: (+86) 21 54741297; Email: yfzhou@sjtu.edu.cn

† Electronic Supplementary Information (ESI) available: details of experiments and characterization, and FT-IR, TEM, DPD, FL and micro-DSC results. See DOI: 10.1039/x0xx00000x

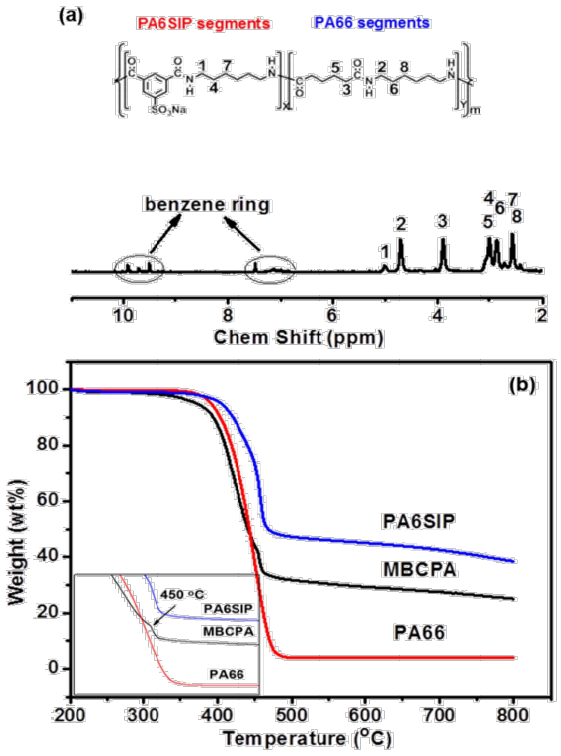

Fig. 1 Characterizations of as-prepared MBCPAs. (a) The NMR spectrum; (b) The TGA curves.

described (Fig. S1, ESI†) by Yamazaki.[10] In the first step, poly (Sodium 5-sulfoisophthalate-alt-hexamethylenediamine) (PA6SIP) and poly (hexanedioic acid-alt-hexamethylenediamine) (PA66) segments were synthesized, respectively; in the second step, the multiblock copolyamide was synthesized by coupling of these two segments. Fig. 1a shows the ^{1}H NMR spectrum of the synthesized MBCPA along with peak assignments in deuterated sulfuric acid. The signals appearing in the region of 6.0-10.0 ppm are ascribed to the protons of benzene ring, and the signals at about 5.0 ppm (peak 1), 4.7 ppm (peak 2) and 3.9 ppm (peak 3) come from the protons adjacent to the amide groups. The chemical shifts below 3.2 ppm are assigned to the methylene moieties (peaks 4-8). Moreover, the peak 2 is an independent signal assigned to the PA66 segments, while the peak 1 is the independent proton signals for PA6SIP segments. The real composition ratio of MBCPA (PA6SIP:PA66) can be obtained according to the integrated areas of peak 1 (S1), peak 2 (S2), and is about 0.35:1. According to Carothers' equation, there should be 4 PA6SIP blocks and 10 PA66 blocks in each MBCPA in theory. So the real composition ratio between PA6SIP and PA66 blocks in MBCPA (0.35:1) is comparable to the theoretic one (0.4:1). The multiblock structure of the synthesized copolyamide was also proved by the thermal gravity analysis (TGA, Fig. 1b), and the TGA curve of MBCPAs shows two stages of evident mass loss at 400 °C due to degradation of the PA66 blocks and at 450 °C due to degradation of the PA6SIP blocks (inset in Fig. 1b).[10] Differential scanning calorimetry (DSC) traces shows two melting peaks around 229 °C and 258 °C for the physical blend of PA66 and PA6SIP, while only one melting peak around 252 °C for MBCPAs, which further ascertain the multiblock structure of MBCPAs (Fig. S4, ESI†). The intrinsic viscosity measured in sulfuric acid (96 wt %) by an Ubbelohde viscometer at 30 °C is

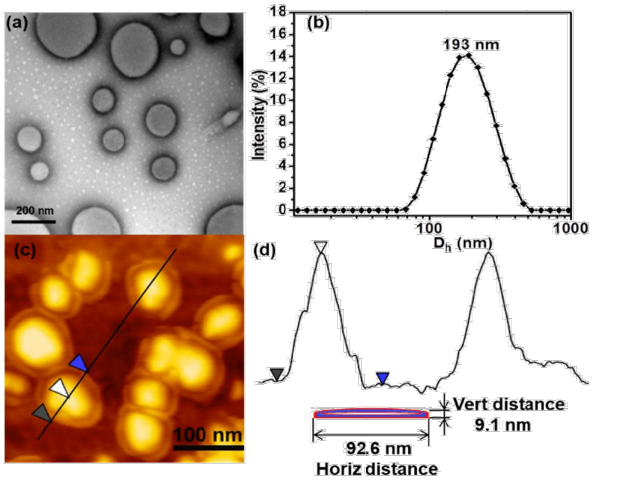

Fig. 2 Morphology characterizations of MBCPA self-assemblies. (a)The TEM image of MBCPA self-assemblies stained by phosphotungstic acid; (b)The DLS curve; (c)The AFM image; (d) The sectional height profiles of the particles and the cartoon to illustrate the cross section of the particles.

1.42, and the viscosity-average molecular weight is about 11,672 according to the semiempirical equation (Fig. S2, ESI†) generated by Ruijter and Picken.[10] The FTIR measurements provide a further evidence to prove the formation of multiblock copolyamides (Fig. S3, ESI†).

In the as-prepared MBCPAs, the PA66 segments are hydrophobic, while the benzene sulfonic acid sodium groups in PA6SIP segments are hydrophilic, so MBCPAs are amphiphilic in nature. Moreover, the amide groups in MBCPAs are subject to form intermolecular hydrogen bonds. So the self-assembly ability of MBCPAs are well expected. To prove this, a direct hydration method by putting polymers into deionized water with a typical concentration of 1 mg/mL was used to trigger the self-assembly process. The transmission electron microscopy (TEM) images (Fig. 2a) show the aggregates are spherical particles with a clear contrast difference between the inner pool and the outer black thin wall. In addition, the particles with holes can also be observed (Fig. S5, ESI†). These results indicate that the aggregates might be vesicles with hollow lumens. The vesicle wall thickness is around 4.3 ± 0.4 nm through the statistical analyses of 30 particles. The dynamic light scattering measurement indicates the vesicles have an average hydrodynamic diameter around 193 nm with a PDI of 0.16 (Fig. 2b). The atomic force microscopy (AFM) image (Fig. 2c) shows collapsed particles with the height-to-diameter ratio more than 1:10, which also proves the formation of vesicles. The height of the collapsed vesicles is around 9 nm, which is equal to the thickness of two stacked vesicle membrane as shown in the cartoon (Fig. 2d). Thus, the vesicle wall thickness measured by TEM is in good agreement with that measured by AFM. The MBCPA vesicles have a polydisperse size distribution according to the TEM, AFM and DLS measurements. In fact, a wide size distribution is often observed for the vesicles self-assembled by a direct hydration method.[11]

The above experiments reveal that the multiblock polyamides could self-assemble into vesicles in aqueous solution, so what is the self-assembly mechanism? To address it, a dissipative particle dynamics simulation was performed to explore the self-

assembly process of the as-prepared MBCPAs. In order to capture the essential feature of MBCPAs, a model molecule $[(AB)_2(CB)_5]_3$ was constructed in the DPD simulations (Fig. 3a). In this system, one "A" bead represents a hydrophilic benzene sulfonic acid sodium group, one "B" bead refers to a hydrophobic hexamethylenediamine group, while one "C" bead refers to a hydrophobic adipic acid group (Fig. 3a). Thus, $(AB)_2$ represents a PA6SIP blocks, while $(CB)_5$ represents a PA66 block. The ratio between AB to CB is 2:5 (0.4:1), which is a mimic of the theoretic composition of MBCPAs. For easy handling, a multiblock polymer with 3 degree of polymerization was constructed in our DPD model. The details of the simulation model and method are described in the Supporting Information. Fig. 3 displays snapshots of the self-assembly process through the DPD simulation. After the initially random state (Fig. 3b), the MBCPA molecules aggregated into a large irregular aggregate with lamellar structure at 66 ns (Fig. 3c). Then, the large irregular aggregate gradually changed to a hollow vesicular shape with several holes throughout the vesicle membrane at 132 ns (Fig. 3d). The vesicle turned more regular with the holes closing from 198 ns (Fig. 3e), 248 ns (Fig. 3f) to 300 ns (Fig. 3g). At t = 792 ns, the vesicle was completely sealed with a regular globular shape (Fig. 3h). Generally, the vesicles from the linear block copolymers can be generated through the mechanisms of "micelle-rod-membrane-vesicles" or "micelle-semivesicle-vesicle".[12] The mechanism of MBCPA vesicles as shown here is closer to the "micelle-rod-membrane-vesicle" process except that no rod-like intermediates are observed, and it is very similar to the vesicle self-assembly mechanism from Janus dendrimers and Janus hyperbranched polymers.[13] During the TEM measurements, some intermediates of lamellar structures, vesicles with two or more holes, and vesicles in closing the holes were also observed (Fig. S6, ESI†), which agree well with the self-assembly pathway as indicated in Fig. 3.

In addition, the simulation results can further provide details on the vesicle structure. Fig. 4a shows that the polymer adopts a core-shell structure with the hydrophilic units on the vesicle shells and with the hydrophobic units inside the vesicle cores. In addition, it can be also seen that the polymer chains display three kinds of packing behaviors in the vesicle membrane (Fig. 4a), namely the folding chains, hanging chains and spanned chains, respectively. For folding chains, the polymer segments do not span the whole vesicle membrane but fold into a "v" type inside the membrane; For spanned chains, the polymer segments do span the whole vesicle membrane; For hanging chains, the polymer segments do not fold and span the vesicle, but just hang in the vesicle membrane. Through the combination of these three packing models, the MBCPAs pack into the vesicles. So, the vesicle is not a simple monolayer or bilayer structure, on the contrary, it is a combination of bilayer and monolayer structure. Such a self-assembly mechanism might be a unique characteristics for multiblock copolymer vesicles when compared to that of the conventional polymersomes and liposomes.[14]

Furthermore, the density distribution from the center of mass to the outside of the vesicle was calculated to characterize the vesicle microstructure. The detailed calculation description can be seen in supporting information. As can be seen in Fig. 4b, the density distribution profile of hydrophilic segments has two peaks while the density distribution profile of two hydrophobic blocks has only one smooth peak, which supports the core-shell structure very well. We can also calculate the membrane thickness of the vesicles from the density distribution profile. The calculated membrane thickness of the vesicle is 4.5 nm, which is very close to the experimental result 4.3 ± 0.4 nm.

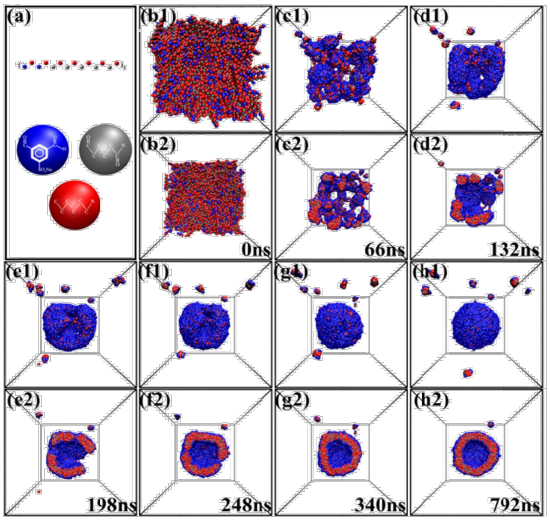

Fig. 3 DPD simulations on the self-assembly of MBCPAs captured at different time intervals. (a) The model $[(AB)_2(CB)_5]_3$ for one MBCPA molecule. (b) Randomly distributed $[(AB)_2(CB)_5]_3$ molecules in water. (c and d) Formation of a large irregular aggregate with the lamellar structure. (e) Formation of a hollow vesicular aggregate with several holes throughout the vesicle membrane. (f and g) The vesicle in closing the holes. (h) The final vesicle structure. For each image from (b–h), the upper one is the 3D view, while the lower one is the cross-section view. The water beads are removed for clarity. Blue: A type bead (benzene sulfonic acid sodium salt block); red: B type bead (hexamethylenediamine block); gray: C type bead (adipic acid block).

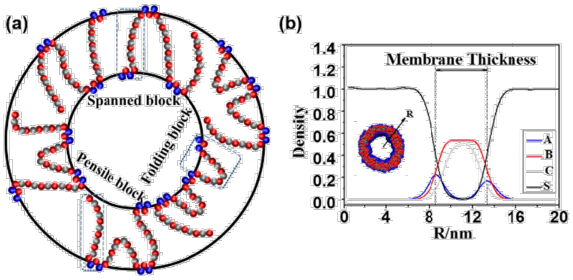

Fig. 4 The vesicular structure by the DPD simulation. (a) The schematic of the packing modes of polymer chains within the vesicle membrane, abd the circle represents the membrane of the vesicle. (b) Radial density distributions of the A (blue), B (red), C (gray) and S (black, solvent particle) components in the vesicle. The distance from the center of mass of the vesicle to the outside of the vesicle is R. Membrane thickness is defined as the distance between the peaks of density distribution of the hydrophilic A segments located on the inside surface and on the outside surface.

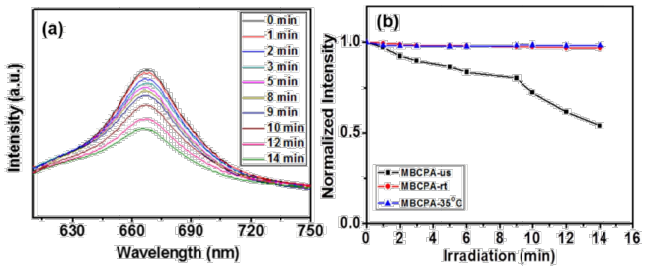

Fig. 5 Ultrasound-responsive dye release experiments from vesicles. (a)The fluorescence emission spectra of NR-loaded MBCPA vesicles (excitation: 600nm) recorded at different ultrasonic irradiation time; (b)The accumulative release of NRs from MBCPA vesicles with (MBCPA-us) or without ultrasonication that performed at room temperature (MBCPA-rt) or at 35 °C (MBCPA-35 °C), respectively.

Generally, the vesicle thickness of polymersomes is around 10-30 nm, while that of the liposomes is around 5 nm or less.[15] Thus, as a kind of polymer vesicles, the wall thickness of 4.5 nm for the obtained MBCPA vesicles is ultrathin. And what's more, there should be a large number of intermolecular hydrogen bonds between amide groups of the synthesized multiblock copolyamides in the vesicles. Thus, we deduce that the vesicles might be disrupted under an external ultrasound stimulus.

As proof-of-principle experiments, the release behaviour of the MBCPA vesicles encapsulated with nile red (NR) was studied under the ultrasound with the power of 150 W and the frequency of 40 KHz. NR can be solubilized in the hydrophobic interiors of the MBCPA vesicles. When the vesicles were disrupted, the encapsulated NR dyes would be released to water to form aggregates, and a quenching of fluorescence could be detected.[16] So, NR can be used as a probe to detect vesicular disruption based on the change of its emitted fluorescence. Fig. 5a shows that the fluorescence intensity of MBCPA vesicles decreases gradually with increasing the cumulative ultrasonic time. There is almost 50% fluorescence decrease after 14 min's ultrasonic irradiation (Fig. 5b). Since the ultrasonication will increase the solution temperature, the ultrasound was stopped for one minute after 30 seconds of irradiation. In addition, some ice was added to prevent the increase of the solution temperature above 35 °C. As the control experiments, almost no fluorescence changes were observed for the NR-loaded MBCPA vesicles in room temperature (Fig. S8, ESI†, Curve MBCPA-rt in Fig. 5b) and at 35 °C (Fig. S8, ESI†, Curve MBCPA-35 °C in Fig. 5b) in the absence of ultrasonic irradiation. Thus, the large decrease in the fluorescence intensity should be attributed to the release of NR dyes from the MBCPA vesicles, that is, the vesicles should be disrupted by the ultrasound. The disruption of MBCPA vesicles by ultrasound was also proved by the TEM measurement (Fig. S9, ESI†). Moreover, to further reveal the uniqueness of ultrasound-responsive behaviour of MBCPA vesicles, another ultrasound release experiment of NR-loaded hyperbranched polymer (HBPO-star-PEO) vesicles was also performed,[17] where HBPO represents the hydrophobic hyperbranched poly(3-ethyl-3-oxetanemethanol) core and PEO represents the hydrophilic poly(ethylene oxide) arm. From Fig. S8c (ESI†), we can find that there is only 5% fluorescence decrease, after 14 mins' ultrasonication, which indicates that the HBPO-star-PEO vesicles are not ultrasound-responsive.

To our knowledge, the MBCPA vesicles reported here represent a new kind of ultrasound-responsive vesicles. The micro differential scanning calorimetry (micro-DSC) and infrared spectroscopy measurements of MBCPA vesicle aqueous solution at a concentration of 1 mg/mL both indicate that the intermolecular hydrogen bonds inside the MBCPA vesicles are broken after ultrasonic irradiation (Figs. S10 and S11, ESI†). This might be the origin of ultrasound stimuli-responsive behaviour of MBCPA vesicles.

Conclusions

In conclusion, herein we have demonstrated the formation of ultrasound responsive vesicles with an ultrathin membrane through the self-assembly of multiblock copolyamides. The computer simulation results have deepened our understanding on the self-assembly pathway of the vesicles which is consistent with the experimental results, and have also demonstrated that the vesicles possess a combined bilayer and monolayer structure. In addition, the origin of the ultrasonic responsivity has been studied, and it is probably due to the break of intermolecular hydrogen bonds inside the vesicles. We believe that the present work has extended the family of polymer vesicles with new structure and property. Furthermore, we expect that the as-prepared ultrasound responsive vesicles might have some application in controlled drug release, and this work is still in progress.

Acknowledgements

We thank the National Basic Research Program (2013CB834506), China National Funds for Distinguished Young Scholar (21225420), the National Natural Science Foundation of China (91527304, 21474062) and "Shu Guang" project supported by Shanghai Municipal Education commission and Shanghai Education Development Foundation (13SG14) for financial support.

Notes and references

1 (a) A. D. Bangham, M. M. Standish and J. C. Watkins, *J. Mol. Biol.*, 1965, **13**, 238; (b) Y. Y. He, Z. B. Li, P. Simone and T. P. Lodge, *J. Am. Chem. Soc.*, 2006, **128**, 2745; (c) J. H. Fendler, *Acc. Chem. Res.*, 1980, **13**, 7; (d) J. M. Gebicki and M. Hicks, *Nature*, 1973, **243**, 232; (e) L. Zhang and A. Eisenberg, *Science*, 1995, **268**, 1728; (f) J. S. Qian, M. Zhang. L, Manners and M. A. Winnik, *Trends Biotechnol.*, 2010, **28**, 84; (g) B. M. Discher, Y.-Y. Won, D. S. Ege, J. C.-M. Lee, F. S. Bates, D. E. Discher and D. A. Hammer, *Science*, 1999, **284**, 1143; (h) P. L. Luisi, P. Walde and T. Oberholzer, *Curr. Opin. Colloid Interface Sci.*, 1999, **4**, 33; (i) X. Guo and F. C. Szoka Jr., *Acc. Chem. Res.*, 2003, **36**, 335.

2 (a) P. L. Soo and A. Eisenberg, *J. Polym. Sci: Polym.*, 2004, **42**, 923; (b) E. W. Kaler, A. K. Murthy, B. E. Rodriguez and J. A. N. Zasadzinski, *Science*, 1989, **245**, 1371; (c) J. C. M. van Hest, D. A. P. Delnoye, M. W. P. L. Baars, M. H. P. van Genderen and E. W. Meijer, *Science*, 1995, **268**, 1592; (d) E. Blasco, J. Serrano, M. Pinol and L. Oriol, *Macromolecules*, 2013, **15**, 5951; (e) L. H. Wang, X. M. Xu, C. Y. Hong, D. C. Wu, Z. Q. Yu and Y. Z. You, *Chem. Commun.*, 2014, **68**, 9676; (f) W. F. Jiang, Y. F.

Zhou and D. Y. Yan, *Chem. Soc. Rev.*, 2015, **12**, 3874; (g) K. C. Jie, Y. J. Zhou, Y. Yao and F. H. Huang, *Chem. Soc. Rev.*, 2015, **44**, 3568; (h) A. K. A. Silva, R. D. Corato, T. Pellegrino, S. Chat, G. Pugliese, N. Luciani, F. Gazeau and C. Wilhelm, *Nanoscale*, 2013, **5**, 11374; (i) Y. Yu, X. G. Jiang, S. Y. Gong, L. Feng, Y. Q. Zhong and Z. Q. Pang, *Nanoscale*, 2014, **6**, 3250.

3 F. S. Bates, M. A. Hillmyer, T. P. Lodge, C. M. Bates, K. T. Delaney and G. H. Fredrickson, *Science*, 2012, **336**, 434.

4 (a) S. Ludwigs, A. Boker, A. Voronov, N. Rehse, R. Magerle and G. Krausch, *Nat. Mater.*, 2003, **2**, 744; (b) C. Ott. R. Hoogenboom, S. Hoeppener, D. Wouters, J. F. Gohy and U. S. Schubert, *Soft Matter*, 2009, **5**, 84; (c) H. Tan, Z. G. Wang, J. H. Li, Z. C. Pan, M. M. Ding and Q. Fu, *ACS Macro Lett.,* 2013, **2**, 146.

5 J. Zhang, Z. Y. Lu and Z. Y. Sun, *Soft Matter*, 2013, **9**, 1947.

6 (a) N. A. Hadjiantoniou, A. I. Triftaridou, D. Kafouris, M. Gradzielski and G. S. Patrickios, *Macromolecules*, 2009, **42**, 5492; (b) S. Y. Ma, M. Y. Xiao and R. Wang, *Langmuir*, 2013, **29**, 16011; (c) A. Halperin, *Macromolecules*, 1991, **24**, 1418.

7 (a) N. A. J. M. Sommerdijk, S. J. Holder, R. C. Hiorns, R. G. Jones and R. J. M. Nolte, *Macromolecules*, 2000, **33**, 8289; (b) M. M. Ding, J. H. Li, X. He, N. J. Song, H. Tan, Y. Zhang, L. Zhou, Q. Gu, H. Deng and Q. Fu, *Adv. Mater.*, 2012, **24**, 3639; (c) L. Q. Yu, L. J. Zhou, M. M. Ding, J. H. Li, H. Tan, Q. Fu and X. L. He, *J. Colloid Interface Sci.*, 2011, **358**, 376; (d) M. M. Ding, X. L. He, L. J. Zhou, J. H. Li, H. Tan, X. T. Fu and Q. J. Fu, *J. Controlled Release*, 2011, **152**, 87; (e) S. J. Holder, R. C. Hiorns, N. A. J. M. Sommerdijk, S. J. Williams, R. G. Jones and R. J. M. Nolte, *Chem. Commun.*, 1998, 1445.

8 (a) J. Z. Du, Y. Q. Tang, A. L. Lewis and S. P. Armes, *J. Am. Chem. Soc.,* 2005, **127**, 17982; (b) S. H. Qin, Y. Geng, D. E. Discher and S. Yang, *Adv, Mater.*, 2006, **18**, 2905. (c) A. Napoli, M. Valentini, N. Tirelli, M. Muller and J. A. Hubbell, *Nat. Mater.*, 2004, **3**, 183; (d) A. C. Coleman, J. M. Belerle, M. C. Stuart, B. Macia, G. Caroli, J. T. Mika, D. J. van Dijken, J. Chen, W. R. Browne and B. L. Feringa, *Nat. Nanotech.*, 2011, **6**, 547; (e) C. W. Lin, Y. H. Chen and W. S. Chen, *J. Med. Ultras*., 2012, **20**, 87; (f) Q. Yan, J. Yuan, Z. Cai, Y. Xin, Y. Kang and Y. Yin, *J. Am. Chem. Soc.,* 2010, **132**, 9268; (g) A. E. Dunn, D. J. Dunn, A. Macmillan, R. Whan, T. Stait-Gardner, W. S. Price, M. Lim and C. Boyer, *Polym. Chem.*, 2014, **5**, 331; (h) B. Karagoz, J. Yeow, L. Esser, S. M. Prakash, R. P. Kuchel, T. P. Davis and C. Boyer, *Langmuir,* 2014, **30**, 10493; (i) T. T. T. N'Guyen, H. T. T. Duong, J. Basuki, V. Montembault, S. Pascual, C. Guibert, J. Fresnais, C. Boyer, M. R. Whittaker, T. P. Davis and L. Fontaine, *Angew. Chem.,* 2013, **125**, 14402.

9 (a) W. Q. Chen and J. Z. Du, *Sci. Rep-UK.,* 2013, **3**, 1; (b) W. Zhou, F. Meng, G. Engbers and J. Feijen, *J. Controlled Release,* 2006, **116**, e62.

10 (a) N. Yamazaki and F. Higashi, *J Poly Sci Part A: Polym. Chem.*, 1974, **12**, 185; (b) C. Ruijer, W. F. Jager, J. Groenewold and S. J. Picken, *Macromolecules*, 2006, **39**, 3826.

11 (a) J. R. Howse, R. A. L. Jones, G. Battaglia, R. E. Ducker, G. L. Leggett and A. J. Ryan, *Nat. Mater.,* 2009, **8**, 507; (b) J. Wang, Y. Z. Ni, W. F. Jiang, H. M. Li, Y. N. Liu, S. L. Lin and Y. F. Zhou, *small*, 2015, **11**, 4485.

12 (a) Y. Y. Han, H. Z. Yu, H. B. Du and W. Jiang, *J. Am. Chem. Soc.,* 2010, **132**, 1144; (b) X. H. He and F. Schmid, *Phys. Rev. Lett.,* 2008, **100**, 137802.

13 (a) V. Percec, D. A. Wilson, P. Leowanawat, C. J. Wilson, A. D. Hughes, M. S. Kaucher, D. A. Hammer, D. H. Levine, A. J. Kim, F. S. Bates, K. P. Davis, T. P. Lodge, M. L. Klein, R. H. DeVane, E. Aqad, B. M. Rosen, A. O. Argintaru, M. J. Sienkowska, K. Rissanen, S. Nummelin and J. Ropponen, *Science*, 2010, **328**, 1009; (b) Y. Liu, C. Y. Yu, H. B. Jin, B. B. Jiang, X. Y. Zhu, Y. F. Zhou, Z. Y. Lu and D. Y. Yan, *J. Am. Chem. Soc.*, 2013, **135**, 4765.

14 (a) D. E. Discher and A. Eisenberg, *Science,* 2002, **297**, 967; (b) M. Antonietti and S. Forster, *Adv. Mater.*, 2003, **15**, 1323; (c) A. Blanazs, S. P. Armes and A. J. Ryan, *Macromol. Rapid Commun.*, 2009, **30**, 267.

15 (a) J. Rodriguez-Hernandez and S. Lecommandoux, *J. Am. Chem. Soc.*, 2005, **127**, 2026; (b) Y. Barenholz, *Curr. Opin. Colloid Interface Sci.*, 2001, **6**, 66; (c) T. Lian and R. J. Y. Ho, *J. Pharm. Sci.,* 2001, **90**, 667.

16 (a) A. P. Goodwin, J. L. Mynar, Y. Ma, G. R. Fleming and J. M. J. Frechet, *J. Am. Chem. Soc.*, 2005, **127**, 9952; (b) J. Xuan, M. Pelletier, H. S. Xia and Y. Zhao, *Macromol. Chem. Phys.*, 2011, **212**, 498.

17 Y. F. Zhou and D. Y. Yan, *Angew. Chem. Int. Ed.*, 2004, **43**, 4896.